Analytic Analysis of Galaxy Number Counts

Master Thesis
by Cynthia Winter

Faculty of Physics,
Bielefeld University

April 2016

Supervisor and First Referee: Prof. Dr. Dominik Schwarz
Second Referee: Dr. Daniel Boriero

Contents

1 Introduction

This master thesis deals with the theoretical investigation and analytical calculation of source counts in different cosmological models. Therefore it is dedicated to the question in how far number counts can be calculated analytically and to what extent they might be used in order to investigate cosmological features, for example the cosmic expansion described by the Hubble law, acceleration or deceleration, spatial curvature and the energy content of the universe which can be composed of various components such as matter, radiation or some kind of dark energy represented by a cosmological constant term in the Friedmann equations.

Number counts of cosmological objects, i.e. galaxies or clusters of galaxies which are gravitationally unbound and thus obeying the Hubble law, are the simplest statistics that can be derived from any survey. Differential number counts correspond to the number of objects in a given flux or redshift interval and solid angle of the sky. Integral source counts are obtained even easier by counting all objects in a given sky area above some minimal flux level or up to the sensitivity reached by the observational instrument. Although integral number counts have been commonly used in the past they have the great disadvantage that rapid changes of the differential number counts are concealed [1]. Furthermore, integral number counts are not statistical independent for different flux densities and estimating errors is difficult (see e.g. [2], [3]).

Contrary to integral counts, differential number counts can be easily applied to test different cosmological models, especially those modelling cosmic evolution of galaxies. For simple models such as the Einstein model, de Sitter model, Einstein-de Sitter and Milne model, number counts can be calculated completely analytical in the case of frequency independent (bolometric) counts. These models also have the great advantage that the number counts can be expressed analytically as a function of flux density instead of redshift. Thus, they could be easily compared to surveys with a vast number of cosmological objects, for no redshift information is necessary which is often unknown for many objects. In the case of frequency dependent source counts, i.e. differential number counts in a given frequency interval, there are still analytic solutions for the number counts expressed redshift dependently, but for the flux dependent counts analytic solutions only exist for some special values of the spectral index α, otherwise approximations have to be made for the low and high redshift regime, respectively.

If combinations of these simple models are considered, e.g. the Λ-Cold-Dark-Matter (ΛCDM) model with flat spatial geometry and an energy density consisting of cold dark matter and dark energy (k=0, $\Omega = \Omega_m + \Omega_\Lambda$) analytic solutions no longer exist, so again approximations are needed or numerical calculations have to be done.

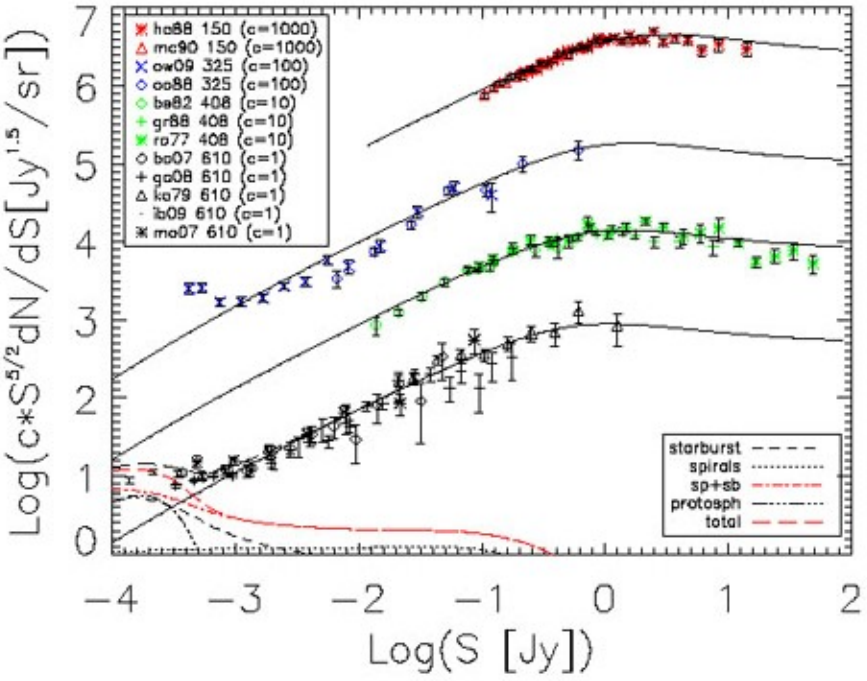

Figure 1.1: Differential source counts at 150, 325, 408, 610 MHz normalised to $cS_\nu^{-2.5}$, with $c = 1000$, 100, 10 and 1, respectively (Figure taken from [4])

The basis for all calculations in this thesis are the Friedmann equations, which are obtained from Einstein's field equations and the Friedmann-Lemaitre-Robertson-Walker (FLRW)-metric, which will be layed out in the second chapter. Sources will be assumed to be point-like with equal luminosities and distributed uniformly throughout space. For the calculation of the differential number counts, first the number of object per solid angle and distance interval is given and then expressed for a redshift interval in the case of expanding models. Then the number counts per solid angle and flux interval are calculated and the result is expressed in terms of the flux. Traditionally, the result is normalised to the source counts expected in a static Euclidean universe for comparison. Comparing the results with data, one would see immediately that evolutionary effects result in a different behaviour than the calculated one, where objects are assumed to be point sources with the same luminosity over all times (e.g. [4]).

Figure 1.1 shows an example of differential number counts data at different frequancies together with fits obtained by an evolutionary model from Massardi et al. [4], [5]. As for this example, number counts are commonly shown in double logarithmic plots as a function of flux density and normalised to $cS_\nu^{-5/2}$.

In the second chapter, a short introduction to the theoretical basis needed for the calculation and interpretation of galaxy number counts is given. This chapter includes the FLRW-metric, the Friedmann equations and cosmological distance measures which have to be applied carefully to avoid ambiguities. Then the general procedure of calculating differential and integral number counts is introduced and carried out in general. Finally, the second chapter concludes with a brief outline of the cosmological models

that will be considered throughout this thesis and some others which are interesting or of historical significance.

In the third chapter, the differential and intergral number counts for the static Euclidean model, static Einstein model, de Sitter, Einstein-de Sitter and Milne model are calculated and compared to each other regarding their special properties such as the limits for the high and low flux regime. Furthermore, the integral number counts will be calculated and the effects of model parameters on the sorce counts will be discussed.

After that, in chapter four, the specific number counts for the expanding models, i.e. the de Sitter model, Einstein-de Sitter and Milne model will be calculated, as the frequency bands are redshifted according to the steepness of the spectrum of the source. Analytic solutions for the frequency dependent case, assuming a spectrum with a constant spectral index α, can only be found for some special values of α, often yielding quite complicated solutions. Therefore a simple but nevertheless accurate approximation for a wide range of fluxes will be given as well and compared to the exact solutions.

Then in the fifth chapter, the number counts for the ΛCDM-model will be considered and calculated analytically as far as possible. There is an analytic solution to the redshift dependent differential number counts, but this cannot be expressed in terms of elementary functions. In order to find a result for the number counts in a flux interval, approximations will be made.

Finally, we will summarise the results and give an outlook on the issues that require further investigation or seem interesting for a better understanding of the way in which features like curvature, energy density and a cosmological constant leave an imprint on cosmology that can be observed via galaxy number counts.

2 Theoretical foundation and cosmological models

2.1 Theoretical foundation

2.1.1 FLRW-metric

The basis for all the following calculations is the Friedmann-Lemaitre-Robertson-Walker-metric (FLRW-metric) which follows from the assumptions of spatial homogeneity and isotropy, i.e. the cosmological principle, which is always assumed throughout this thesis. In its most general form the FLRW-metric reads

$$ds^2 = -dt^2 + a(t)^2 d\Sigma^2 \tag{2.1}$$

(where the speed of light is set equal to 1). For simplicity in the calculations for $d\Sigma^2$ the following convention

$$d\Sigma^2 = d\chi^2 + f^2(\chi) d\Omega^2 \tag{2.2}$$

is used and thus the FLRW-metric is given by

$$ds^2 = -dt^2 + a^2(t) \left(d\chi^2 + f^2(\chi) d\Omega^2 \right), \tag{2.3}$$

where

$$f(\chi) = \begin{cases} \frac{1}{\sqrt{k}} \sin(\sqrt{k} \cdot \chi) & : \quad k = +1 \\ \chi & : \quad k = 0 \\ \frac{1}{\sqrt{|k|}} \sinh(\sqrt{|k|} \cdot \chi) & : \quad k = -1 \end{cases} \tag{2.4}$$

with $d\Omega^2 = d\theta^2 + \sin^2(\theta) d\phi^2$ and $\chi = f^{-1}(r)$ and the curvature parameter k = +1, 0 and -1 standing for positive spatial curvature (spherically, closed universe), zero curvature (open, flat space) and negatively curved space (hyperbolic, open universe), respectively. The FLRW-metric can also be expressed in terms of the radial distance r as

$$ds^2 = -dt^2 + a^2(t) \left(\frac{dr^2}{1 - kr^2} + r^2 d\Omega^2 \right) \tag{2.5}$$

[2]. There are two different conventions regarding the FLRW-metric. On one hand, the curvature can be taken to be dimensionless with the discrete values $k = 0, \pm 1$. Then the distance χ is also dimensionless and the scale factor must have dimensions of length. On the other hand, the curvature can be taken to have the dimension of $1/[length]^2$, then the scale factor is dimensionless. Throughout this thesis the first convention will be applied.

2.1.2 Friedmann equations

All cosmological models considered in this thesis are based on the Friedmann equations which are obtained by applying the FLRW-metric to Einstein's field equation of general relativity (see e.g. [6]). The first Friedmann equation

$$H^2 + \frac{k}{a^2} = \frac{8\pi G}{3}\rho + \frac{\Lambda}{3} \tag{2.6}$$

is derived from the 00-component of Einstein's equation. Here H(t) is the Hubble parameter

$$H(t) = \frac{\dot{a}(t)}{a(t)}, \tag{2.7}$$

k the curvature parameter, G the gravitational constant, Λ the cosmological constant and $\rho = \rho(t)$ denotes the total energy density of the universe at cosmic time t. From the first Friedmann equation together with the trace of Einstein's field equation follows the second Friedmann equation, often also referred to as the Friedmann acceleration equation

$$\dot{H} + H^2 = \frac{\ddot{a}}{a} = -\frac{4\pi G}{3}(\rho + 3p) + \frac{\Lambda}{3}, \tag{2.8}$$

where p denotes the pressure. For the energy density and the pressure it holds the cosmological equation of state of a perfect fluid

$$w = \frac{p}{\rho} \tag{2.9}$$

where w is assumed dimensionless. When applied to the FLRW-metric, the equation of state describes the cosmic evolution of a perfect fluid in an isotropic universe. Regarding the covariant energy-momentum conservation equation

$$\dot{\rho} = -3(\rho + p)\frac{\dot{a}}{a} \tag{2.10}$$

and assuming that w is a constant, the equation of state can be related with the scale factor via

$$\rho \propto a^{-3(1+w)}. \tag{2.11}$$

These equations will be used in order to derive the properties of the various cosmological models for different curvature and energy contents. Once the main features of a cosmological model like curvature, cosmological constant and energy density are specified, the Friedmann equations can be used to calculate the other properties such as the Hubble parameter and scale factor.

2.1.3 Distance measures

In cosmology there exist different distance measures according to the way in which the issue is considered. Because of the curvature of space-time there is no unambiguous distance that can always be applied, but these distance measures become equal to the Euclidean notion of distance for redshifts close to one. Regarding cosmological

distances the central assumption which is made is that all observers have the same cosmic age.

One of the most important distance measures in cosmology is the redshift z for which holds

$$1 + z = \frac{a_0}{a}, \tag{2.12}$$

where a_0 denotes the present value of the scale factor [7].

A useful distance measure for the calculation of the differential number counts in flat models is the Hubble distance

$$d_H = \frac{1}{H(z)}, \tag{2.13}$$

which corresponds to the age the universe would have if the expansion had been linear in the past.

The distance which corresponds to the 'real' distance between objects is the so called proper distance, which is the coordinate distance times the scale factor, i.e.

$$d_p(t) = a \int_0^{\chi} d\chi' = a\chi. \tag{2.14}$$

For an observed light ray ($ds^2 = 0$) it follows from the FLRW-metric

$$-\frac{dt}{a(t)} = d\chi \tag{2.15}$$

and the redshift changes with time like

$$\frac{dz}{dt} = \frac{d(1+z)}{dt} = \frac{d(a_0/a)}{dt} = -(1+z)H(z). \tag{2.16}$$

Therefore the coordinate distance is given by

$$\chi = \int_t^{t_0} \frac{dt}{a} = -\frac{1}{a_0} \int_z^0 \frac{1+z'}{(1+z')H(z')} dz' \tag{2.17}$$

and thus the comoving distance becomes

$$d_c(z) = a_0\chi = \int_0^z \frac{dz'}{H(z')}. \tag{2.18}$$

Then the proper distance becomes equal to

$$d_p(z) = \frac{a}{a_0} d_c(z) = \frac{d_c(z)}{1+z}. \tag{2.19}$$

Another important distance measure is the luminosity distance d_L which is given by

$$d_L = \sqrt{\frac{L}{4\pi S}} = \sqrt{\frac{P}{S}}. \tag{2.20}$$

The luminosity distance is relevant for obtaining the flux of an object depending on its redshift and will be used for the calculation of the number counts expressed in terms of the flux. The flux is given by

$$S = \frac{L}{4\pi a_0^2 (1+z)^2 f^2(\chi)} = \frac{P}{(1+z)^2 a_0^2 f^2(\chi)} \tag{2.21}$$

and therefore the luminosity distance for arbitrary curvature becomes

$$d_L(z) = (1+z) a_0 f(\chi) = (1+z) a_0 f\left(\frac{d_c}{a_0}\right) \tag{2.22}$$

with

$$f(\chi) = \frac{1}{\sqrt{k}} \sin\left(\sqrt{k}\chi\right). \tag{2.23}$$

Thus the luminosity distance can be expressed as

$$d_L(z) = (1+z)\sqrt{\frac{a_0^2}{k}} \sin\left(\sqrt{\frac{k}{a_0^2}} d_c(z)\right). \tag{2.24}$$

In flat space, the luminosity distance becomes

$$d_L = (1+z) d_c. \tag{2.25}$$

Furthermore, another distance measure is the angular diameter distance

$$d_a(z) = \frac{R_p(z)}{\theta} = a(t) f(\chi) = a_0 \frac{1}{1+z} f(\chi) = a_0 \frac{1}{1+z} f\left(\frac{d_c}{a_0}\right) \tag{2.26}$$

which relates the actual diameter of an object $R_p(z)$ to its angular diameter θ. With the luminosity distance the angular diameter distance can be expressed as

$$d_a(z) = \frac{1}{(1+z)^2} d_L(z). \tag{2.27}$$

This distance measure is not needed for the calculations of differential number counts in this thesis but nonetheless stated here for the sake of completeness.

2.1.4 Differential number counts

Like already mentioned in the previous chapter, differential or integral number counts are a very simple and practical means for validating cosmological models and screening the history of the universe. In order to calculate the number counts, the properties of the different cosmological models are applied to the Friedmann equations to derive the unknown parameters which then can be used to obtain the Hubble distance and the comoving distance. Differential number counts are defined as the number of objects (meaning galaxies or galaxy clusters) in a solid angle $d\Omega$ and a distance interval dr or more general $d\chi$, i.e.

$$\frac{dN}{d\Omega d\chi}.$$

Since the coordinate distance χ is not an observable quantity and radial distances are hard to obtain especially for very distant objects, it is more convenient to write the number counts for a redshift interval dz

$$\frac{dN}{d\Omega dz} = \frac{dN}{d\Omega d\chi}\frac{d\chi}{dz}. \tag{2.28}$$

As redshift information is also not available for many objects, it is often more practical to rewrite the differential number counts for a flux interval rather than redshift as fluxes can be "easily" measured. Therefore the quantity

$$\frac{dN}{d\Omega dS} = \frac{dN}{d\Omega dz}\frac{dz}{dS} \tag{2.29}$$

should be established.

The calculation of differential number counts begins with the FLRW-metric (see sec. 2.1.1), from which the volume in the solid angle $d\Omega$ and coordinate distance interval $d\chi$ can be derived as

$$\frac{dV}{d\Omega d\chi} = a^3 f^2(\chi) = \frac{a_0^3 f^2(\chi)}{(1+z)^2}. \tag{2.30}$$

With equation (2.12) for the redshift, equation (2.18) and

$$n(z) = n_0(1+z)^3, \tag{2.31}$$

the differential number counts in a solid angle $d\Omega$ and coordinate distance interval $d\chi$ become

$$\frac{dN}{d\Omega d\chi} = n_0 a_0^3 f^2\left(\frac{d_c(z)}{a_0}\right). \tag{2.32}$$

The change of the redshift with the coordinate distance is given by

$$\frac{dz}{d\chi} = \frac{dz}{dt}\frac{dt}{d\chi} = (1+z)H(z)\frac{a_0}{1+z} = a_0 H(z). \tag{2.33}$$

As the quantity χ cannot be measured it is more convenient to calculate either the differential number counts for a redshift or for a flux interval. The differential number counts in a redshift interval dz are given by

$$\frac{dN}{d\Omega dz} = n_0 a_0^2 f^2\left(\frac{d_c(z)}{a_0}\right)\frac{1}{H(z)}. \tag{2.34}$$

Then the differential number counts can be expressed as a function of redshift by

$$\frac{dN}{d\Omega dz} = n_0\frac{a_0^2}{k}\sin^2\left(\sqrt{\frac{k}{a_0^2}}d_c(z)\right)\frac{1}{H(z)}. \tag{2.35}$$

Accordingly, the differential number counts for a flux interval dS can be calculated using equation (2.29). Together with equation (2.22) and equation (2.34) the general solution for the differential number counts in a frequency interval dS is given by

$$\frac{dN}{d\Omega dS} = -\frac{n_0}{2P}\frac{f^5\left(\frac{d_c}{a_0}\right)(1+z)^3}{f\left(\frac{d_c}{a_0}\right) + \frac{df\left(\frac{d_c}{a_0}\right)}{dz}(1+z)}\frac{1}{H(z)}. \tag{2.36}$$

As the calculation of this expression is much simpler using the model dependent solutions of the differential number counts in the redshift interval $\frac{dN}{d\Omega dz}$ and the changing rate of the flux with redshift $\frac{dS}{dz}$, the quantity $\frac{dN}{d\Omega dS}$ will be calculated for each model separately in the third chapter via equation (2.29).

Differential number counts probe the evolution of the comoving volume and a possible evolution of the sources, i.e. $n_0 = n_0(z)$. Unfortunately, for distant objects there is a strong correlation of the number counts to evolution of the sources, i.e. the evolution of galaxies both in number (galaxies have merged in the past) and their luminosity (galaxies have been more luminous in the past) (e.g. [4]]. Therefore catalogues of very distant galaxies cannot be directly applied to the calculated differential number count without evolutionary models being taken into account.

2.1.5 Integral number counts

Another cosmological probe is provided by integral number counts, that is the total number of galaxies above a given flux limit

$$\frac{dN}{d\Omega}(> S_{min}) = \int_{S_{min}}^{\infty} \frac{dN}{d\Omega dS} dS, \tag{2.37}$$

or up to a given value of redshift

$$\frac{dN}{d\Omega}(< z_{max}) = \int_{0}^{z_{max}} \frac{dN}{d\Omega dz} dz. \tag{2.38}$$

Integral number counts have the disadvantage of concealing changes in the number density with the flux. Furthermore the numbers of sources in two neighbouring flux intervals are not statistically independent from each other. Although integral number counts are impractical as a cosmological probe for a comparison of models with data, they can be quite useful for a comparison of different models and their properties, assuming all objects are identical.

2.2 Cosmological models

All cosmological models considered thoughout this thesis are Friedmann models, which means based on the Friedmann equations and thus on general relativity. As the Friedmann equations are derived from Einstein's field equation together with the FLRW-metric (see section 2.1), Friedmann models also include the cosmological principle, that is the assumption of homogeneity and isotropy (e.g. [6]).

The first necessary step for deriving a simple model of the universe and its possible evolution in time, is the cosmological principle, for this gives the simple FLRW-metric. Accordingly, the Hubble law must be valid, because it is the unique expansion law which conserves homogeneity and isotropy (e.g. [12]). Historically, the first attempt in finding a reasonable model for the universe, was to assume that everything was static, for this would simplify the matter enourmously as distances and objects never changed.

Therefore the simplest cosmological model that can be considered is the static Euclidean universe. This universe is flat and neither expanding nor contracting and thus space just corresponds to the three-dimensional Euclidean space. That leads to the differential number counts being proportional to $(S/S_0)^{5/2}$. This model traditionally serves as a reference for all other models. Moreover, the Euclidean part can be isolated from the flux dependent differential number counts in all models considered in the third chapter and therefore the remaining factor can be examined seperately. Unfortunately, a static Euclidean universe can only be realized in a spatially infinite and empty universe.

Furthermore, a reaonable cosmological model should be compatible with general relativity and therefore Einstein's field equations. This is how the static Einstein model and with it the cosmological constant came about. Einstein wanted to install a model of the universe which was both static (temporally infinite) and spatially finite, but to counteract the gravitational attraction of matter he had to propose a cosmological constant keeping a spatially finite universe from collapsing or expanding. Moreover, this model is closed, hence having a spherical spatial geometry with k=+1. The energy density only consists of pressureless "dust" and the cosmological constant, the Hubble rate and redshift are of course zero in a static universe and thus the scale factor is constant ($a = a_0$). Unfortunately, this model is highly unstable because even very slight deviations from the right energy density and cosmological constant or spatial curvature lead to an expanding or contracting universe (see e.g. [8], [9]).

At that time, also another static model was proposed which would also be static with a Euclidean geometry. This model is spatially as well as temporally infinite, thus not needing a cosmological constant to counteract gravity, and also spatially flat. As this universe is of infinite age and size the light of infinitely many stars had time to reach the earth and therefore would lead to a bright night sky in contradiction to observation, known as Olbers' paradox.

Another stationary cosmology which was quite popular before the discovery of the cosmic microwave background is the steady state model proposed by Hoyle, Bondi and Gold in 1948 [10], [11]. In this model the universe actually is expanding to account for the observed redshift behaviour described by the Hubble law, but the so called 'perfect cosmological principle' holds which states that besides being isotropic and homogeneous the universe also never changes its appearance throughout time. Therefore this model requires a continuous production of matter in order to maintain a constant matter density and thus constant star formation rates. Furthermore, in the steady state model there has to be a mechanism to transform or destroy the material of burned-out stars or supernova remnants etc. keeping the number density of these objects constant as well. This model resembles a de Sitter universe with its constant Hubble rate and constant energy density instead of a cosmological constant. As this model has been ruled out in favor of the big bang model, it will not be considered any further in this thesis.

The de Sitter model is a flat model with a constant Hubble rate and constant energy density which is represented only by the cosmological constant term in the Friedmann equations. A constant Hubble rate leads to an exponentially accelerated expansion. As the universe at its current age seems to be at a transition between a matter dominated and a cosmological constant dominated era, the de Sitter universe is an interesting model to be considered. Actually, the two other cases with positive and negative

spatial curvature, i.e. $k = \pm 1$ are also referred to as de Sitter models, but will not be considered in this thesis, as the Hubble rate is not constant any more and given by a more complicated expression than for the simpler models (see e.g. [12]).

An example of a simple matter dominated cosmological model is the Einstein-de Sitter model (e.g. [13]). Like the de Sitter model considered before it is spatially flat ($k = 0$) without a cosmological constant ($\Lambda = 0$) and therefore the first Friedmann equation simplifies to $H^2 = \frac{8\pi G}{3}\rho$. For a matter dominated universe the expansion rate is given by the Hubble law $H = H_0(1+z)^{3/2}$ and the energy density is equal to the critical energy density which is needed to have an expansion big enough to avoid a gravitational collapse. This means that the expansion of the Einstein-De Sitter model is slowed down more and more due to gravity but will never cease. The Einstein-de Sitter model is a very practical model to describe the expansion history of the universe since radiation pressure became irrelevant for cosmic evolution and before the accelerated expansion due to some unknown (dark) energy began.

To account for a universe with hyperbolic space, the Milne model is also considered in this thesis. The Milne model is an empty universe, i.e. with zero energy density and hyperbolic spatial geometry ($k = -1$). As there is no space-time curvature due to either matter or a cosmological constant it holds the flat Minkowski space-time for the Milne model and therefore special relativity. Thus it is the only simple Friedmann model with a constant, i.e. linear expansion with $H = H_0(1+z)$. Because of its missing energy density the Milne model clearly is no reasonable cosmological model but still worth to consider for investigating the effects of hyperbolic space on a cosmological model (see e.g. [12], [14]).

The most interesting of the models considered throughout this thesis is the cold dark matter model with dark energy or cosmological constant, the ΛCDM model, as it is the standard cosmological model. For simplicity the radiation component is left out to enable a slightly simpler calculation of the differential number counts. This ΛCDM model is spatially flat and the Hubble rate is given by $H = H_0\sqrt{\Omega_m(1+z)^3 + \Omega_\Lambda}$ with $\Omega_m + \Omega_\Lambda = 1$ if radiation is neglected, where Ω_m and Ω_Λ denote the ratios of the energy density of matter and dark energy to the total energy density of the universe, respectively see e.g. [6]. The calculation of differential number counts for this model already is quite difficult, as the comoving distance which corresponds to the integral of the inverse Hubble rate has no solution that can be expressed in terms of elemantary functions but contains hypergeometric functions. An analytic solution can still be found for differential number counts given redshift dependently, but the flux dependent differential number counts cannot be solved analytically any more. Therefore approximations become necessary for the calculation of the differential number counts in the ΛCDM model.

For the sake of completeness it must be stated that there are still other interesting cosmological models but most of these are no Friedmann models, i.e. models which are not isotropic or without constant curvature everywhere. Additionally, there are cosmologies for which other models of gravity than the theory of general relativity are assumed, such as modified Newtonian gravity or a gravitational constand which is changing with time.

3 Bolometric differential number counts

3.1 Calculation of the differential number counts

In the following section the differential number counts will be calculated under the assumptions that all objects are point-like, have the same luminosity and are uniformly distributed throughout the universe. Furthermore, it is assumed for simplicity that the total flux can be measured over all frequencies (bolometric). Another assumption that will be made for all calculations throughout this thesis is of course that features like spatial curvature and physical laws are the same everywhere and for every time.

3.1.1 Static Euclidean universe

The by far simplest model for which differential number counts can be calculated is the static Euclidean universe. For the calculation, a flat space without any evolution and a uniformly distributed number of luminous objects being stars or galaxies is assumed. As the model is assumed to be static, no dynamics due to gravitational attraction must be taken into account. This model could clearly only be realised when the universe is both spatially and temporally infinite.

Because there is no curvature at all and also no expansion or contraction of space, everything can be desribed in terms of Euclidean distances. Therefore the number of objects inside a shell of a sphere around the observer in the distance r and solid angle of the sky Ω is given by

$$\frac{dN}{d\Omega dr} = n_0 a_0^3 r^2. \tag{3.1}$$

Then for the flux an observer on the earth would measure from a point like source in the radial distance $a_0 r$ it holds

$$S = \frac{P}{a_0^2 r^2}. \tag{3.2}$$

Therefore the differential number counts in a flux interval become

$$\frac{dN}{d\Omega dS} = \frac{dN}{d\Omega dr}\frac{dr}{dS} = -\frac{n_0 a_0^5}{2P} r^5. \tag{3.3}$$

With the substitution

$$r = \frac{1}{a_0}\sqrt{\frac{P}{S}} \tag{3.4}$$

the Euclidean flux dependent differential number counts become

$$\frac{dN}{d\Omega dS} = -\frac{n_0}{2P}\left(\frac{P}{S}\right)^{5/2}. \tag{3.5}$$

Finally, in order to enable a comparison with the other models considered in the following sections the differential number counts can be expressed for the flux normalized to S_0 as

$$\frac{dN}{d\Omega d(S/S_0)} = -\frac{N_0}{2}\left(\frac{S}{S_0}\right)^{-5/2}, \tag{3.6}$$

by setting $S_0 = P/a_0^2$ and $N_0 = n_0 a_0^3$.

3.1.2 Static Einstein model

As already mentioned in the previous chapter, Einstein's cosmological model is static ($H = 0, z = 0, a = a_0$), spherically closed ($k = +1$) and the energy density consists of pressureless matter and the cosmological constant. According to equation (2.32) in the previous chapter and $f = \sin(\chi)$ for $k = +1$, the differential number counts in the solid angle $d\Omega$ and coordinate distance interval $d\chi$ for the Einstein model are given by

$$\frac{dN}{d\Omega d\chi} = n_0 a_0^3 \sin^2(\chi). \tag{3.7}$$

With equation (2.22) and $z = 0$ for static models it holds for the flux

$$S = \frac{P}{a_0^2 \sin^2(\chi)}. \tag{3.8}$$

The changing rate of the flux with coordinate distance is calculated as

$$\frac{dS}{d\chi} = -\frac{2P}{a_0^2 \sin^3(\chi)}\cos(\chi) \tag{3.9}$$

and thus according to equation (2.29) the differential number counts in a solid angle $d\Omega$ and flux interval dS yield

$$\frac{dN}{d\Omega dS} = -\frac{n_0 a_0^5}{2P}\frac{\sin^5(\chi)}{\cos(\chi)}. \tag{3.10}$$

From equation (3.8) it follows

$$\sin(\chi) = \frac{1}{a_0}\sqrt{\frac{P}{S}} = \sqrt{\frac{S_0}{S}} \tag{3.11}$$

and for $\chi \in [0, \pi]$ it holds

$$\cos(\chi) = \sqrt{1 - \frac{S_0}{S}}. \tag{3.12}$$

Thus the differential number counts can be written as

$$\frac{dN}{d\Omega dS} = -\frac{n_0 a_0^5}{2P}\left(\frac{S}{S_0}\right)^{-5/2}\frac{1}{\sqrt{1 - \frac{S_0}{S}}}. \tag{3.13}$$

For a better comparison with the expanding models and cancelling out the power this can be expressed in terms of the dimensionless parameter S/S_0 as will be done for

the other models below. Setting $S_0 = P/a_0^2$ and $N_0 = n_0 a_0^3$ as for the Euclidean model it holds

$$\frac{dN}{d\Omega d(S/S_0)} = -\frac{N_0}{2}\left(\frac{S}{S_0}\right)^{-5/2}\frac{1}{\sqrt{1-\frac{1}{S/S_0}}}. \tag{3.14}$$

This result yields the same formula as for the number counts in a static Euclidean universe with an additional factor of $1/\sqrt{1-S_0/S}$ resulting from the positive curvature of the static Einstein model. From equation (3.12) it folllows that $0 \leq \sqrt{1-\frac{S_0}{S}} \geq 1$ and thus $S \geq S_0$.

According to this result, the differential number counts in the static Einstein model agree with the Euclidean number density for high flux densities and grow like $1/\sqrt{1-S_0/S}$ for decreasing flux. There is a singular point at $S = S_0$, which corresponds to the "equator" of the 3- sphere. However, this is not problematic if $dN/d\Omega$ is finite.

3.1.3 De Sitter model

The de Sitter universe is a cosmological model whose evolution is only determined by a constant energy density, i.e. a cosmological constant which drives an exponential expansion. Additionally it is spatially flat and has a constant Hubble rate ($k = 0$, $H = H_0$, $\rho = \rho_\Lambda = \frac{H_0^2}{4\pi G}$ from the Friedmann equations). This model has got some relevance for the future evolution of the universe, since it is known that a transition between a matter dominated and cosmological constant dominated universe is taking place.

Because the de Sitter model is spatially flat we have $f(\chi) = \chi$ [see.eq. (2.4) and eq. (2.18)] and therefore the differential number counts in a distance interval $d\chi$ become

$$\frac{dN}{d\Omega d\chi} = a_0^3 \chi^2 n_0. \tag{3.15}$$

With the general result from equation (2.34) the differential number counts in a solid angle $d\Omega$ and redshift interval dz can be directly given as

$$\frac{dN}{d\Omega dz} = \frac{n_0 a_0^2 \chi^2}{H(z)} = \frac{n_0 a_0^2 \chi^2}{H_0}. \tag{3.16}$$

According to equation (2.18) and equation (2.22) for the flux in the de Sitter model it holds

$$S = \frac{P}{d_L^2} = \frac{P}{d_c^2(1+z)^2} = \frac{P H_0^2}{z^2(1+z)^2}. \tag{3.17}$$

In order to obtain the differential number counts in the solid angle $d\Omega$ and flux interval dS via equation (2.29) the changing rate of the flux with redshift has to be calculated which yields

$$\frac{dS}{dz} = -\frac{2PH_0^2(1+2z)}{(z+z^2)^3}. \tag{3.18}$$

Therefore the differential number counts for the de Sitter model become

$$\frac{dN}{d\Omega dS} = -\frac{n_0}{2PH_0^5}\frac{z^5(1+z)^3}{1+2z}. \tag{3.19}$$

To eliminate the redshift from this formula the equation for the flux is solved for the redshift yielding

$$z = -\frac{1}{2} + \sqrt{\frac{1}{4} + H_0\sqrt{\frac{P}{S}}} \tag{3.20}$$

and then inserted in $\frac{dN}{d\Omega dS}$ which becomes

$$\frac{dN}{d\Omega dS} = -\frac{n_0}{4PH_0^5}\frac{\left(H_0\sqrt{\frac{P}{S}}\right)^3\left(\sqrt{\frac{1}{4}+H_0\sqrt{\frac{P}{S}}}-\frac{1}{2}\right)^2}{\sqrt{\frac{1}{4}+H_0\sqrt{\frac{P}{S}}}}. \tag{3.21}$$

As for the other models we express this equation in terms of S/S_0 in order to obtain an equation containing a constant prefactor with the parameters which are not specified by the model, i.e. the number density and current Hubble rate, times a constant and a power law part with the argument S/S_0 and some constants depending on the model. Then the formula for the differential number counts be rearranged yielding an expression containing the Euclidean factor $(S/S_0)^{-5/2}$

$$\frac{dN}{d\Omega d(S/S_0)} = -2N_0\frac{\left(\frac{S}{S_0}\right)^{-5/2}}{\sqrt{1+4\left(\frac{S}{S_0}\right)^{-1/2}}\left(\sqrt{1+4\left(\frac{S}{S_0}\right)^{-1/2}}+1\right)^2}, \tag{3.22}$$

with $S_0 = PH_0^2$ and $N_0 = n_0/H_0^3$. Considering the limits for the high and low flux regime i.e. for low and high values of redshift, respectively, yields the same power law for low redshifts as for Einstein's static universe (and a static Euclidean model); for large redshifts (low fluxes), S/S_0 goes with the power of -7/4 (for a comparison of the limits see section 3.2).

3.1.4 Einstein-de Sitter model

The Einstein-de Sitter universe is a matter dominated model with flat spatial geometry and no cosmological constant ($k = 0$, $\Lambda = 0$, $\rho = \frac{3H^2}{8\pi G}$). Contrary to the static Euclidean universe, static Einstein model and the de Sitter universe, this model has no constant energy density because there is a certain amount of matter which dilutes with the expansion of the universe depending on the Hubble rate. In this special case of a matter dominated universe in flat space, the energy density of the universe corresponds to the critical density that has just the right value to counteract gravitational attraction. Thus, the universe will expand forever but at an ever decreasing rate.

Regarding the Friedmann equations and properties of the Einstein-de Sitter model, the Hubble rate is given by

$$H(z) = H_0(1+z)^{3/2} \tag{3.23}$$

and therefore with equation (2.18) the comoving distance becomes

$$d_c = \frac{2}{H_0}\left(1 - \frac{1}{\sqrt{1+z}}\right). \tag{3.24}$$

According to these results together with equation (2.34), the differential number counts in the solid angle $d\Omega$ and redshift interval dz for the Einstein-de Sitter model yield

$$\frac{dN}{d\Omega dz} = \frac{4n_0}{H_0^3}\frac{\left(1 - \frac{1}{\sqrt{1+z}}\right)^2}{(1+z)^{3/2}}. \tag{3.25}$$

With the comoving distance calculated above and equation (2.22) for the flux in the Einstein-de Sitter model it holds

$$S = \frac{H_0^2 P}{4\left(1+z-\sqrt{1+z}\right)^2}. \tag{3.26}$$

As a next step again the derivative dS/dz is calculated which gives

$$\frac{dS}{dz} = -\frac{H_0^2 P}{4}\frac{2\sqrt{1+z}-1}{(1+z)^2(\sqrt{1+z}-1)^3}. \tag{3.27}$$

Thus $\frac{dN}{d\Omega dS}$ becomes

$$\frac{dN}{d\Omega dz}\frac{dz}{dS} = -\frac{16n_0}{H_0^5 P} \quad \frac{(\sqrt{1+z}-1)^5}{(2\sqrt{1+z}-1)\sqrt{1+z}}. \tag{3.28}$$

Like for the de Sitter model the equation for the flux is solved for 1+z to be inserted in the above formula. This yields the following expression for the redshift

$$\sqrt{1+z} = \frac{1}{2} + \frac{1}{2}\sqrt{1 + 2H_0\sqrt{\frac{P}{S}}}. \tag{3.29}$$

Inserting this result for $1+z$ in the formula for the differential number counts it holds

$$\frac{dN}{d\Omega dS} = -\frac{16n_0}{H_0^5 P} \quad \frac{\left(\frac{1}{2}\sqrt{1+2H_0\sqrt{\frac{P}{S}}} - \frac{1}{2}\right)^5}{\left(\sqrt{1+2H_0\sqrt{\frac{P}{S}}}\right)\left(\frac{1}{2}\sqrt{1+2H_0\sqrt{\frac{P}{S}}} + \frac{1}{2}\right)}. \tag{3.30}$$

Again, as for the de Sitter model, $H_0^2 P$ is substituted with S_0 to obtain an equation whose power law part depends on S/S_0

$$\frac{dN}{d\Omega d(S/S_0)} = -32N_0\frac{\left(\frac{S}{S_0}\right)^{-5/2}}{\sqrt{1+2\left(\frac{S}{S_0}\right)^{-1/2}}\left(\sqrt{1+2\left(\frac{S}{S_0}\right)^{-1/2}}+1\right)^6}, \tag{3.31}$$

where $N_0 = n_0/H_0^3$. Considering the limit for $S/S_0 \gg 1 \quad (z \ll 1)$, the differential number counts match the result $\frac{dN}{d\Omega d(S/S_0)} = -\frac{n_0}{2H_0^3}(S/S_0)^{-5/2}$ of the static Euclidean universe, while the limit for $S/S_0 \ll 1 \quad (z \gg 1)$ evolves like $(S/S_0)^{-3/4}$. This means that the Einstein-de Sitter model must have expanded faster than the de Sitter model to counteract the gravitational attraction of matter and reach the current Hubble parameter.

3.1.5 Milne model

Another interesting case is the Milne model, which is an empty universe, i.e. with no energy density or cosmological constant but in hyperbolic space ($k = -1$, $\Lambda = 0$, $\rho = 0$ and $H = -\frac{k}{a^2} = \frac{1}{a^2}$). Therefore this cosmology can be used to study the properties of a hyperbolic spatial geometry. Furthermore, it is the only model which grows linear with time (i.e. the scale factor a(t) is linear in t), which means that the deceleration parameter is zero. Because of $\rho = 0$ and $\Lambda = 0$, the first Friedmann equation for the Milne model reads

$$H^2 = -\frac{k}{a^2}. \tag{3.32}$$

and with $H = \frac{\dot{a}}{a}$ this becomes

$$H^2 = H_0^2 \frac{a_0^2}{a^2} = -\frac{k}{a^2} \tag{3.33}$$

and thus $k = -H_0^2 a_0^2 = -1$. The Hubble rate in the Milne model is given by

$$H(z) = H_0(1+z) \tag{3.34}$$

in the Milne model and therefore

$$d_c = \frac{\ln(1+z)}{H_0} \tag{3.35}$$

and

$$\chi = H_0 d_c = \ln(1+z). \tag{3.36}$$

With equation (2.23), $\chi = \ln(1+z)$ and using $a_0^2 = 1/H_0^2$, the differential number counts in solid angle $d\Omega$ and redshift interval dz in the Milne model are given by

$$\frac{dN}{d\Omega dz} = \frac{n_0}{H_0^3} \frac{\sinh^2(\ln(1+z))}{1+z} = \frac{n_0}{4H_0^3} \frac{\left((1+z)^2 - 1\right)^2}{(1+z)^3}. \tag{3.37}$$

As a next step, the differential number counts for a flux interval dS are calculated via equation (2.29) by inserting the inverse of dS/dz. According to equation (2.22) and using $a_0^2 = 1/H_0^2$ again, the flux in the Milne model is given by

$$S = \frac{P H_0^2}{\sinh^2(\ln(1+z))(1+z)^2} \tag{3.38}$$

so the derivative becomes

$$\frac{dS}{dz} = -16 P H_0^2 \frac{1+z}{\left((1+z)^2 - 1\right)^3}. \tag{3.39}$$

Regarding these results for the flux dependent differential number counts it holds

$$\frac{dN}{d\Omega dS} = -\frac{n_0}{64PH_0^5}\frac{((1+z)^2-1)^5}{(1+z)^4}. \tag{3.40}$$

For the purpose of eliminating the redshift from the differential number counts formula, again the equation for the flux is solved for $1+z$ yielding

$$1+z = \sqrt{2\sqrt{\frac{PH_0^2}{S}}+1} \tag{3.41}$$

and the result inserted in the differential number counts

$$\frac{dN}{d\Omega dS} = -\frac{n_0}{2PH_0^5}\frac{\left(\frac{PH_0^2}{S}\right)^{5/2}}{\left(2\sqrt{\frac{PH_0^2}{S}}+1\right)^2}. \tag{3.42}$$

Finally this is expressed for S/S_0 by inserting $S_0 = PH_0^2$ in this formula and using $N_0 = n_0/H_0^3$. Therefore the differential number counts in the solid angle $d\Omega$ and $d(S/S_0)$ are given by

$$\frac{dN}{d\Omega d(S/S_0)} = -\frac{N_0}{2}\frac{\left(\frac{S}{S_0}\right)^{-5/2}}{\left(2\left(\frac{S}{S_0}\right)^{-1/2}+1\right)^2}. \tag{3.43}$$

Hyperbolic space, i.e. negatively curved space, is responsible for a constant expansion without any acceleration or deceleration. For high fluxes (low redshifts), the differential number counts have the Euclidean limit which is proportional to $(S/S_0)^{-5/2}$ as for the other models before. The limit for low fluxes (high redshifts) is proportional to $(S/S_0)^{-3/2}$. Therefore the differential number counts in the Molne model are closer to that of the de Sitter model than the Einstein-de Sitter model. Obviously, models with no energy density contributed by matter had slower expansion rates in the past than the matter dominated Einstein-de Sitter universe.

As the the cosmic expansion is only driven by a hyperbolically curved space, Milne originally suggested, that the starting point of the universe could be modelled like a 'real' initial explosion of matter in an empty space being described in a special relativistic manner only (see e.g. [12], [14]). This is of course problematic because that matter would also contribute to a further space-time curvature making such a modelling valid only for very small matter contents where the effects of general relativity can be neglected.

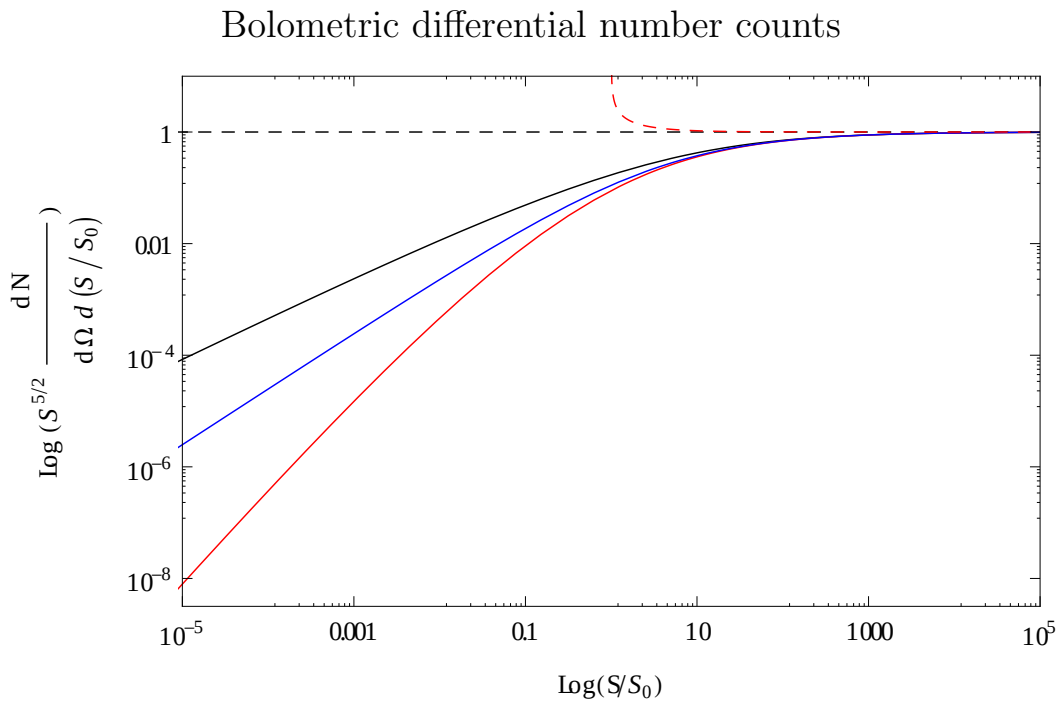

Figure 3.1: Differential bolometric number counts normalised to 1 for $S/S_0 \gg 1$. Black, dashed: static Euclidean universe, red,dashed: Einstein model , black: flat de Sitter model, blue: Milne model, red: Einstein-de Sitter model.

3.2 Comparison of the models

3.2.1 Comparison of the the differential number counts

In this section, we will investigate, which properties of cosmological models can be actually seen regarding number counts. This leads to the question to what extent number counts provide a useful and meaningful cosmological test which can be applied for validating cosmological models or deriving their parameters.

The most obvious feature is that number counts model the volume of the universe. Therefore they are a probe of cosmic expansion and can be used to track the history of the universe. Furthermore we will investigate in this section if and how the other parameters of the different models such as curvature, energy density and a cosmological constant leave an imprint on differential number counts and thus might be used in order to validate the standard ΛCDM model or contrary to this for deriving the current values of the Hubble rate and other parameters.

The differential number counts are usually normalized to the static Euclidean counts and weighted, i.e. multiplied by $c \cdot (S/S_0)^{5/2}$, giving the current number density of galaxies in the universe for $S/S_0 \gg 1$. Here, the differential number counts have been normalised to one for high flux densities using $c = -2/N_0$. Then the number counts are displayed in a double logarithmic plot so that the graphs of the various models show "linear" behaviour for large redshifts and then tilt to today's value for large flux densities. In figure 3.1, the Euclidean normalised bolometric differential number counts for the five models calculated above are shown.

Table 3.2: Limits for $S/S_0 \gg 1$ and $S/S_0 \ll 1$

Model	$S/S_0 \ll 1$	$S/S_0 \gg 1$
Euclidean	$-\frac{N_0}{2}\left(\frac{S}{S_0}\right)^{-5/2}$	$-\frac{N_0}{2}\left(\frac{S}{S_0}\right)^{-5/2}$
De Sitter	$-\frac{N_0}{4}\left(\frac{S}{S_0}\right)^{-7/4}$	$-\frac{N_0}{2}\left(\frac{S}{S_0}\right)^{-5/2}$
Einstein-de Sitter	$-\sqrt{8}N_0\left(\frac{S}{S_0}\right)^{-3/4}$	$-\frac{N_0}{2}\left(\frac{S}{S_0}\right)^{-5/2}$
Milne	$-\frac{N_0}{8}\left(\frac{S}{S_0}\right)^{-3/2}$	$-\frac{N_0}{2}\left(\frac{S}{S_0}\right)^{-5/2}$

Table 3.1: Bolometric differential number counts $\frac{dN}{d\Omega d(S/S_0)}$

Model	$\frac{dN}{d\Omega d\left(\frac{S}{S_0}\right)}$
Euclidean	$-\frac{N_0}{2}\left(\frac{S}{S_0}\right)^{-5/2}$
Einstein	$-\frac{N_0}{2}\left(\frac{S}{S_0}\right)^{-5/2}\frac{1}{\sqrt{1-\frac{1}{S/S_0}}}, \qquad S > S_0$
De Sitter	$-\frac{N_0}{4}\left(\frac{S}{S_0}\right)^{-5/2}\frac{1}{\sqrt{1+4\left(\frac{S}{S_0}\right)^{-1/2}}\left(\sqrt{1+4\left(\frac{S}{S_0}\right)^{-1/2}}+1\right)^2}$
Einstein-de Sitter	$-32N_0\left(\frac{S}{S_0}\right)^{-5/2}\frac{1}{\sqrt{1+2\left(\frac{S}{S_0}\right)^{-1/2}}\left(\sqrt{1+2\left(\frac{S}{S_0}\right)^{-1/2}}+1\right)^6}$
Milne	$-\frac{N_0}{2}\left(\frac{S}{S_0}\right)^{-5/2}\frac{1}{\left(2\left(\frac{S}{S_0}\right)^{-1/2}+1\right)^2}$

For a better comparison of the models considered before, the results for the differential number counts and limits for $S/S_0 \gg 1$ and $S/S_0 \ll 1$ are given in tables 3.1 and 3.2.

As already mentioned previously, these graphs show in the first place how the differential number counts and therefore the proper volume must have behaved in the past for the different cosmological models to lead to the number density observed today in the nearby universe for high fluxes i.e. low redshifts. Figure 3.1 shows that the flat de Sitter model is the one with the slowest expansion of the non static models. In order to reach the current value of the number density of galaxies in the universe, the de Sitter model needed more time than the matter dominated Einstein-de Sitter universe and must therefore be older. The Einstein-de Sitter model must have expanded much

faster than the de Sitter model at early times, because it only consists of pressureless matter, thus the fast expansion is needed to avoid a contraction due to gravity. In the Milne model, there is no energy density present, so the only source of 'expansion' would be the negative curvature of space. This shows that negative curvature resembles an expansion which has been somewhat faster than for a cosmological constant dominated universe, which is not surprising regarding the Hubble rates being $H = H_0$ for the de Sitter universe and $H = H_0(1+z)$ for the Milne model. The fact that the graph for the Einstein-de Sitter model is much steeper than for the other expanding models indicates that the behaviour of the differntial number counts in $d(S/S_0)$ is not just dominated by the expansion of space which is characterised by the Hubble law as $H = H_0(1+z)^{3/2}$ only has an additional factor of $\sqrt{1+z}$ compared to the Milne model.

3.2.2 Effects of model parameters on number counts

In this section the effects that other combinations of the parameters in the Friedmann equations i.e. curvature, a cosmological constant and matter would have on the cosmic expansion and therefore on differential number counts will be discussed. As the differential number counts model the expansion of the proper volume with redshift or flux, the expansion rate, i.e. the Hubble rate has the a greatest effect on the number counts. Therefore it can be used to investigate the behaviour of such models qualitatively.

Regarding the first Friedmann equation (2.6), it becomes obvious that the only case for a contracting universe is a positively curved space together with the combination of matter and cosmological constant being smaller than $\frac{k}{a^2}$. Of the flat models, the slowest expanding model would be the de Sitter model because the cosmological constant must be very small to lead to the current value of the Hubble parameter, whereas the matter dominated case would have expanded fastest in the past to overcome gravity. The combination of matter and a cosmological constant must be between the two other cases to meet the observed value of the number density of sources today. A combination of negative curvature, matter and a cosmological constant would lead to the fastest expansion which can be described by a Friedmann model, because $1/a^2$ is added to the Hubble rate and the scale factor is positive.

Furthermore, a consideration of equation (2.36) shows that besides the Hubble rate via the function $f(\chi)$ the curvature affects the differential number counts in $d\Omega d(S/S_0)$ as well. Moreover, it follows from the Friedmann equations that the curvature also has an effect on the Hubble rate. The effect of curvature on the differential number counts in a flux interval dS is quite complicated because it is contained in equation (2.36) as a function of the coordinate distance χ which could be expressed as $\chi = d_c/a_0$ and therefore contains the integral over the Hubble rate (see eq. (2.18)).

3.2.3 Integral number counts

Although integral number counts have several disadvantages compared to differential counts as mentioned in the introduction, they can still be useful for constraining the parameters. The integral number counts are defined as the total number of objects above a given flux density (see sec 2.1.4). Because calculations become rather complicated for some of the models, we will calculate the the number of objects for $S > S_0$,

Table 3.3: Bolometric integral number counts

Model	$\int_{S_0}^{\infty} \frac{dN}{d\Omega d(S/S_0)} d(S/S_0)$	
De Sitter	$\frac{\sqrt{5}-2}{3} N_0$	$\approx 0,079 N_0$
Einstein-de Sitter	$\frac{8(26-15\sqrt{3})}{3} N_0$	$\approx 0,051 N_0$
Milne	$\left(\frac{ln(27)-4}{12}\right) N_0$	$\approx 0,059 N_0$

i.e. the integral over the differential number counts from the reference flux S_0 to infinity

$$\int_{S_0}^{\infty} \frac{dN}{d\Omega d\left(\frac{S}{S_0}\right)} dS. \tag{3.44}$$

Then by inserting the upper limit one term becomes zero thus giving simple expressions only consisting of the lower limit of the integration S_0 multiplied by a constant factor. This gives the expressions for the integral number counts in the models calculated above as displayed in table 3.3.

These values show how the total numbers of objects above a given flux limit deviate from each other in the different models. This shows that the integral number counts in the three expanding models is of the same order of magnitude. Furthermore, the values of integral number counts for the Einstein-de Sitter model and the Milne model are closer together than the de Sitter model and the Milne model, although these are more similar in the differential number counts plotted in the previous section. Inserting the current number density of objects for negligible redshifts and the current value of the Hubble parameter H_0, the total numbers of objects above a given flux could be directly compared with the observed values. Anyway, this would certainly not be reasonable as these are the results for bolometric number counts and we have assumed that all sources have the same luminosity.

4 Frequency dependent number counts

In the previous chapter, bolometric differential number counts have been calculated analytically for several cosmological models. As observations can only be made in a certain frequency band due to instrumental restrictions it is more convenient to calculate the differential number counts as a function of frequency, i.e. for a "straight" spectrum characterised by its spectral index α. The frequency of light is then redshifted by cosmic expansion and therefore shifted into another frequency interval by an additional factor of $(1+z)^{-\alpha}$. Accordingly, this correction must be taken into account for the calculations when the redshift dependent number counts shall be expressed in terms of a frequency interval dS.

There exist special values of the spectral index besides the bolometric case, for which the differential number counts $\frac{dN}{d\Omega d(S/S_0)}$ have analytic solutions and thus can be compared to the approximations that become necessary for arbitrary values of α. Evidently, the correction for the flux is only needed for non-stationary cosmological models and therefore the static Euclidean universe and static Einstein universe are excluded here.

For the calculation of frequency dependent number counts the results for the redshift dependent differential number counts $\frac{dN}{d\Omega dz}$ can be taken from the third chapter, as the total number of objects in a redshift interval dz remains unchanged. The shifting of the spectra to lower energies due to the expansion of space must be taken into account for the determination of the flux that reaches the earth in a certain frequency and redshift interval dS/dz. As typical radio sources have very "straight" spectra the luminosity in proportional to

$$P(\nu) \propto \nu^{-\alpha} \tag{4.1}$$

leading to the following equation for the flux

$$S_\nu = \frac{P}{a_0^2 f^2(\chi)(1+z)^{1+\alpha}}. \tag{4.2}$$

In order to obtain the differential number counts in a flux interval $\frac{dN}{d\Omega dS}$, first the derivative dS/dz must be calculated which can be done analytically for arbitrary values of α and inserted in equation (2.29). Then, like for the bolometric calculations in the previous chapter, the equation for the flux must be solved for the redshift z which can now only be carried out analytically for certain values of the spectral index.

As in the third chapter, the differential number counts are shown S/S_0-dependently in a double logarithmic plot, where the number counts are normalised to the Euclidean case, i.e. multiplied with a constant and $S^{5/2}$ such that $\frac{dN}{d\Omega d(S/S_0)}$ is one for $S/S_0 \gg 1$.

4.1 Exact solutions

4.1.1 De Sitter model

In the de Sitter model the luminosity distance is equal to the comoving distance because of spatial flatness, therefore

For flat models we have $a_0 f(\chi) = d_c$ and therefore the flux for the de Sitter model is given by

$$S_\nu = \frac{P}{d_c^2 (1+z)^{1+\alpha}} \tag{4.3}$$

and with $d_c = \frac{z}{H_0}$ this becomes

$$S_\nu = \frac{P H_0^2}{z^2 (1+z)^{1+\alpha}}. \tag{4.4}$$

In the limit $S \gg S_0$ the redshift is approximately $z \approx 1/\sqrt{S/S_0}$ for arbitrary α, which is in agreement with the Euclidean result. The changing rate of the flux with redshift is given by

$$\frac{dS_\nu}{dz} = -P H_0^2 \left(\frac{z(3+\alpha)+2}{z^3 (1+z)^{2+\alpha}} \right). \tag{4.5}$$

For the differential number counts in the de Sitter model in a solid angle $d\Omega$ and redshift interval dz we had

$$\frac{dN}{d\Omega dz} = n_0 d_H d_c^2 = \frac{n_0 z^2}{H_0^3} \tag{4.6}$$

and thus the differential number counts in $d\Omega dS_\nu$ become

$$\frac{dN}{d\Omega dS_\nu} = -\frac{n_0}{P H_0^5} \frac{z^5 (1+z)^{2+\alpha}}{z(3+\alpha)+2}. \tag{4.7}$$

There exist quite simple solutions for some integer values of α and furthermore there are solutions for other values of the spectral index like for $1/2$ which yield very complicated expressions and therefore will not be given here. Quite simple solutions can be found for $\alpha = 0$ and $\alpha = 3$; for $\alpha = 2$ there is no analytic solution for the redshift z. Other simple expressions can be found for negative spectral indices $\alpha = -1, -2, -3$. These solutions are

$\alpha = 0$:

$$\begin{aligned} z &= \frac{2^{1/3}}{3\left(3\sqrt{3}\sqrt{27\left(\frac{S_0}{S_\nu}\right)^2 - 4\frac{S_0}{S_\nu}} + 27\frac{S_0}{S_\nu} - 2\right)^{1/3}} \\ &+ \frac{\left(3\sqrt{3}\sqrt{27\left(\frac{S_0}{S_\nu}\right)^2 - 4\frac{S_0}{S_\nu}} + 27\frac{S_0}{S_\nu} - 2\right)^{1/3}}{3 \cdot 2^{1/3}} - \frac{1}{3} \end{aligned} \tag{4.8}$$

$\alpha = 1$ (bolometric case):

$$z = \sqrt{\sqrt{\frac{S_0}{S_\nu}} + \frac{1}{4}} - \frac{1}{2} \tag{4.9}$$

and $\alpha = 3$:

$$\begin{aligned} z &= \frac{2^{1/3}}{3\left(3\sqrt{3}\sqrt{27\frac{S_0}{S_\nu} - 4\sqrt{\frac{S_0}{S_\nu}}} - 27\frac{S_0}{S_\nu} + 2\right)^{1/3}} \\ &+ \frac{\left(3\sqrt{3}\sqrt{27\frac{S_0}{S_\nu} - 4\sqrt{\frac{S_0}{S_\nu}}} - 27\frac{S_0}{S_\nu} + 2\right)^{1/3}}{3 \cdot 2^{1/3}} - \frac{2}{3}. \end{aligned} \tag{4.10}$$

There also exist exact solutions for negative values of the spectral index; the solutions for $\alpha = -1, -2$ and -3 are given below. According to the Rayleigh-Jeans law we have for flux density in the regime of low frequencies $S \propto T\nu^2$, i.e. the case $\alpha = -2$ corresponds to thermal sources.

$\alpha = -1$:

$$z = \sqrt{\frac{S_0}{S_\nu}} \tag{4.11}$$

$\alpha = -2$:

$$z = \frac{1}{2}\left(\frac{S_0}{S_\nu} + \sqrt{\frac{S_0}{S_\nu}\left(\frac{S_0}{S_\nu} + 4\right)}\right) \tag{4.12}$$

$\alpha = -3$

$$z = \frac{\sqrt{\frac{S_0}{S_\nu}} - \frac{S_0}{S_\nu}}{\frac{S_0}{S_\nu} - 1} \tag{4.13}$$

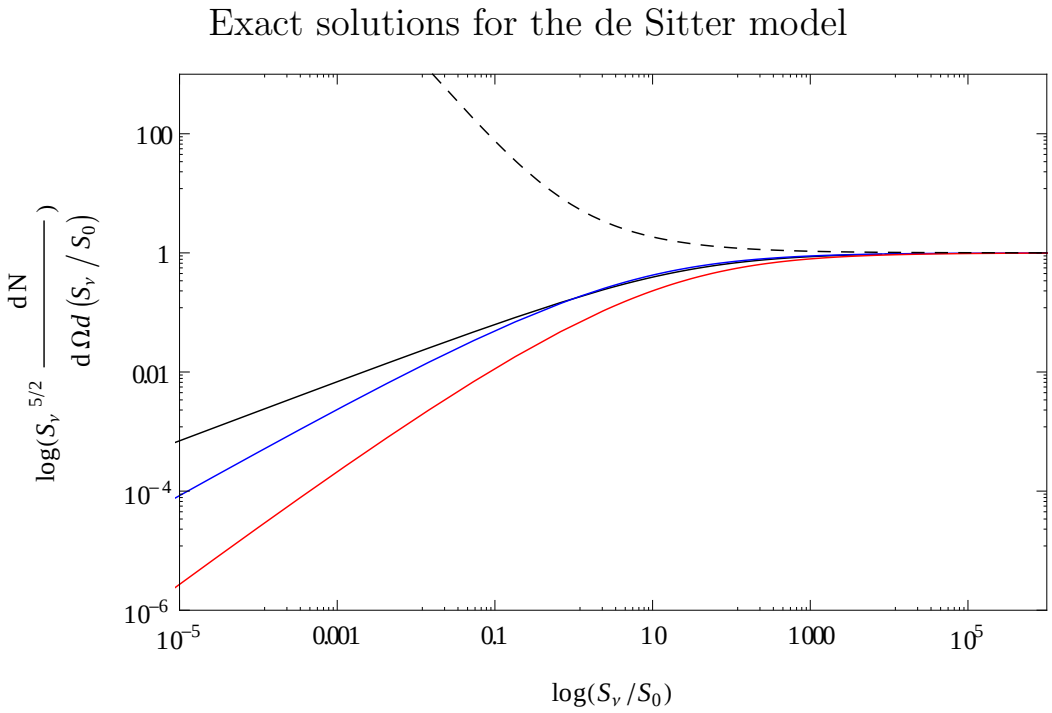

Figure 4.1: Exact solutions of the specific differential number counts for the de Sitter model. Dashed: $\alpha = -2$, black: $\alpha = 0$, blue: $\alpha = 1$ (bolometric solution), red: $\alpha = 3$.

Figure 4.1 shows the differential number counts for the values of $\alpha = -2, 0, 1, 3$ normalised to one for $S/S_0 \gg 1$. Obviously, a steeper spectrum of the source leads to a steeper slope of the differential number counts for small flux densities. This behaviour is not surprising as one might expect a greater change in the luminosity from one frequency interval to the next to result in a larger difference of the redshifting of these frequencies. As we will see in the case of the Einstein-de Sitter model, this assumption must be wrong because there the steepest of the graphs at low flux densities is the one which corresponds to the smallest spectral index. This must be due to the fact that there are two opposing mechanisms: on the one hand, we have an increasing number density for decreasing flux density, but on the other hand the frequencies are redshifted to ever lower values leading to a higher number of objects in this regime. Therefore it depends on the sign of the spectral index wether the differential number counts increase or decrease for small flux densities.

4.1.2 Einstein-de Sitter model

Like the de Sitter model, the Einstein-de Sitter model is flat and therefore it holds $a_0\chi = d_c$. The comoving distance in the Einstein-de Sitter model was given in equation (3.24). Then the equation for the flux becomes

$$S_\nu = \frac{PH_0^2}{4\left(\sqrt{1+z}-1\right)^2(1+z)^\alpha}. \tag{4.14}$$

The changing rate of the flux with redshift is given by

$$\frac{dS_\nu}{dz} = -\frac{PH_0^2}{4} \quad \frac{(1+\alpha)\sqrt{1+z}-\alpha}{(1+z)^{1+\alpha}\left(\sqrt{1+z}-1\right)^3} \tag{4.15}$$

and therefore it holds for the flux dependent differential number counts expressed z-dependently

$$\frac{dN}{d\Omega dS_\nu} = -\frac{16n_0}{PH_0^5} \quad \frac{\left(\sqrt{1+z}-1\right)^5(1+z)^{-3/2+\alpha}}{\sqrt{1+z}(1+\alpha)-\alpha}. \tag{4.16}$$

As for the flat de Sitter model considered in the previous section there are some special values of the spectral index α for which the flux can be solved analytically for the redshift. The results for these values of α which yield rather simple expressions for the redshift depending on the flux are given in the following (where $S_0 = PH_0^2$):

$\alpha = 0$:

$$1+z = \left(\sqrt{\frac{S_0}{4S_\nu}}+1\right)^2 \tag{4.17}$$

$\alpha = 1/2$:

$$1+z = \frac{1}{2}\left(1+2\frac{S_0}{4S_\nu}+\sqrt{4\frac{S_0}{3S_\nu}+1}\right) \tag{4.18}$$

$\alpha = 1$ (bolometric):

$$1+z = \left(\frac{1}{2}+\sqrt{\frac{1}{4}+\sqrt{\frac{S_0}{4S_\nu}}}\right)^2 \tag{4.19}$$

$\alpha = 2$:

$$\begin{aligned} 1+z &= \frac{1}{3} \\ &- \frac{2^{1/3}\left(-3\sqrt{\frac{S_0}{S_\nu}}-1\right)}{3\left(2+3\sqrt{3}\sqrt{\frac{27}{16}\left(\frac{S_0}{S_\nu}\right)^2+\frac{1}{2}\left(\frac{S_0}{S_\nu}\right)^{3/2}}+\frac{27}{4}\frac{S_0}{S_\nu}+9\sqrt{\frac{S_0}{S_\nu}}\right)^{1/3}} \\ &+ \frac{\left(2+3\sqrt{3}\sqrt{\frac{27}{16}\left(\frac{S_0}{S_\nu}\right)^2+\frac{1}{2}\left(\frac{S_0}{S_\nu}\right)^{3/2}}+\frac{27}{4}\frac{S_0}{S_\nu}+9\sqrt{\frac{S_0}{S_\nu}}\right)^{1/3}}{3\cdot 2^{1/3}} \end{aligned} \tag{4.20}$$

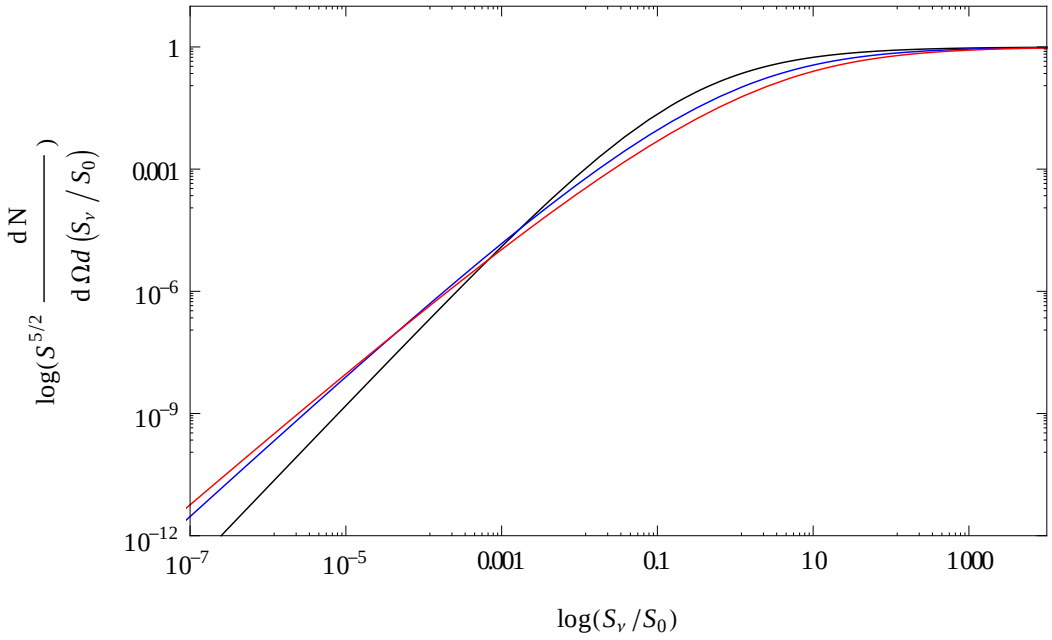

Figure 4.2: Exact solutions of the specific differential number counts for the Einstein-de Sitter model. Black: $\alpha = 0$, blue: $\alpha = 1$ (bolometric solution), red: $\alpha = 2$.

$\alpha = -1/2$:

$$1 + z = \frac{1}{2}\left(\frac{S_0}{4S_\nu}\left(\frac{S_0}{4S_\nu} + 4\right) + \sqrt{\frac{S_0}{4S_\nu}}\left(\frac{S_0}{4S_\nu} + 2\right)\sqrt{\frac{S_0}{4S_\nu} + 4}\right). \tag{4.21}$$

and $\alpha = -2$:

$$1 + z = \frac{S_\nu}{S_0}\left(1 + \sqrt{1 - \frac{2}{\sqrt{S_\nu/S_0}}}\right)^2. \tag{4.22}$$

Figure 4.2 shows the frequency dependent differential number counts for the Einstein-de Sitter model for $\alpha = 0, 1, 2$. In comparison to the de Sitter model, the order of the graphs is inverted. This contradicts the naive assumption that steeper spectra lead to steeper number counts as stated in the previous section. This is of course right for the redshift dependent number counts in a flux interval dS, but it is the redshift-dependence on the flux which leads to this inversion of the graphs. Like it was said in the previous section, the number of objects grows for decreasing flux densities but simultaneously the frequencies are redshifted more and more as the flux density decreases. Furthermore, the Einstein-de Sitter model has a decelerated expansion and therefore the expansion rate must have been very high at low frequencies. Accordingly, in the case of the Einstein-de Sitter model a steeper spectrum of sources results in a flatter graph for the flux dependent differential number counts.

4.1.3 Milne model

The frequency dependent flux in the Milne model is given by

$$S_\nu = \frac{PH_0^2}{\sinh^2\left(\ln(1+z)\right)(1+z)^{1+\alpha}} = \frac{4PH_0^2}{(1+z)^{-1+\alpha}\left((1+z)^2-1\right)^2} \tag{4.23}$$

and therefore

$$\frac{dS_\nu}{dz} = 4PH_0^2(1-\alpha)(1+z)^{2-\alpha}\frac{1-\frac{1}{(1+z)^2}-\frac{4}{1-\alpha}}{\left((1+z)^2-1\right)^3}. \tag{4.24}$$

Thus, the differential number counts become

$$\frac{dN}{d\Omega dS_\nu} = \frac{n_0}{16PH_0^5} \quad \frac{\left((1+z)^2-1\right)^5}{(1+z)^{5-\alpha}\left(1-\alpha-\frac{1-\alpha}{(1+z)^2}-4\right)}. \tag{4.25}$$

Then the exact solutions that exist for certain values of the spectral index α are given below.

There is a solution for $\alpha = 0$ but it is a very complicated expression and therefore not given here explicitly but the result for the differential number counts for a zero spectral index is shown in figure 4.3.

$\alpha = 1$ (bolometric):

$$1+z = \sqrt{\frac{4S_0}{S_\nu}+1}. \tag{4.26}$$

The equation for the flux can be solved analytically for $\alpha = 2$ as well but this yields a very complicated expression which is also not given here explicitly for that reason.

$\alpha = 3$:

$$1+z = \frac{\sqrt{1+\sqrt{1+4\frac{4S_0}{S_\nu}}}}{\sqrt{2}} \tag{4.27}$$

$\alpha = -1$:

$$1+z = \frac{\sqrt{\frac{4S_0}{S_\nu}+4\sqrt{\frac{S_0}{S_\nu}+1}\sqrt{\frac{S_0}{S_\nu}}+2}}{\sqrt{2}} \tag{4.28}$$

There are also a few other values for which the flux can be solved for the redshift analytically, e.g. $\alpha = -2$, but the results are quite complicated and therefore excluded here. Still, the frequency dependent results can be used to investigate in which way the spectral index influences the behaviour of differential number counts for different cosmological models.

The flux dependent differential number counts show a similiar correlation to the spectral index α as for the de Sitter model which means that a greater value of α leads to a steeper graph in the Euclidean normalised double logarithmic plot.

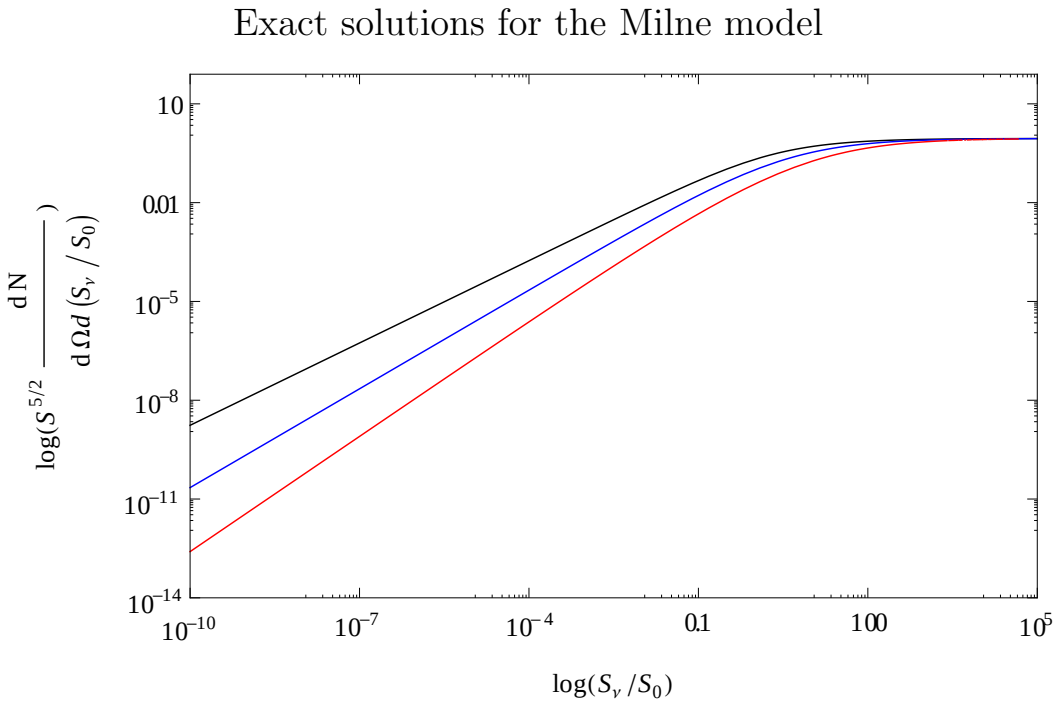

Figure 4.3: Exact solutions of the specific differential number counts for the Milne model. Black: $\alpha = 0$, blue: $\alpha = 1$ (bolometric solution), red: $\alpha = 3$.

4.2 Approximations

After investigating for which values of the sprectral index α the differential number counts can be calculated analytically in the previous section, this section serves the purpose of finding general solutions for arbitrary values of α for the number counts of the models considered before. The main problem regarding the calculation of number counts is expressing the equation for the flux as a function of redshift in order to insert the result in $\frac{dN}{d\Omega dS}(z)$. As the flux cannot be solved for the redhift analytically for arbitrary values of the spectral index α, approximations have to be made. Obviously, the simplest way of finding approximations is to consider the limits of high and low redshifts, i.e. low and high fluxes which will be done in this section.

4.2.1 De Sitter model

The differential number counts per solid angle $d\Omega$ and flux interval dS_ν expressed in terms of the redshift have been calculated analytically in section 4.1.1 yielding equation (4.31). Now the flux equation must be solved for z or $1+z$ and inserted in equation (4.3) in order to obtain the specific differential number counts for a spectral index α.

For high redshifts, i.e. low flux, it holds

$$\lim_{z\to\infty} z^2(1+z)^{1+\alpha} = z^{3+\alpha}, \tag{4.29}$$

which yields

$$\frac{PH_0^2}{S_\nu} \approx z^{3+\alpha}. \tag{4.30}$$

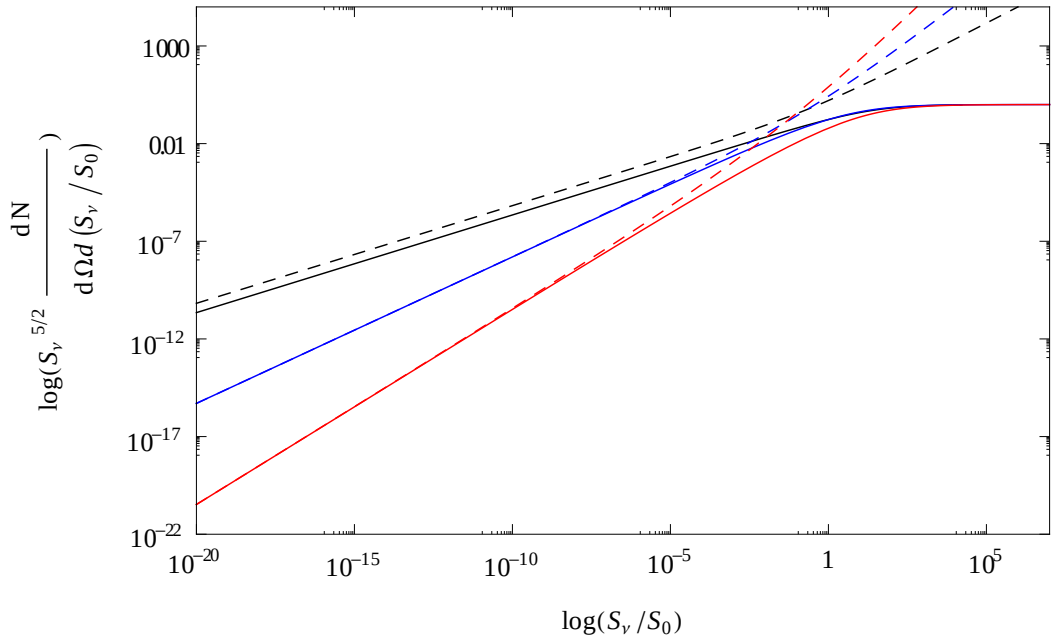

Figure 4.4: Exact solutions and approximations of the specific differential number counts for the de Sitter model for $S_\nu/S_0 \ll 1$. Solid lines are the exact solutions, dashed lines the approximations.
Black: $\alpha = 0$, blue: $\alpha = 1$ (bolometric solution), red: $\alpha = 3$.

Therefore in the limit $z \gg 1$ the redshift depends on the flux as

$$z \approx \left(\frac{PH_0^2}{S_\nu}\right)^{\frac{1}{3+\alpha}}. \tag{4.31}$$

Inserting this result in equation (4.6) and expressing it in terms of the non redshifted flux S_0, the approximated specific differential number counts for low fluxes become

$$\frac{dN}{d\Omega d(S_\nu/S_0)} \approx -\frac{n_0}{H_0^3} \quad \frac{\left(\frac{S_\nu}{S_0}\right)^{-\frac{5}{3+\alpha}} \left(\left(\frac{S_\nu}{S_0}\right)^{-\frac{1}{3+\alpha}} + 1\right)^{2+\alpha}}{(3+\alpha)\left(\frac{S_\nu}{S_0}\right)^{-\frac{1}{3+\alpha}} + 2}. \tag{4.32}$$

For low redshifts, that is in the limit $z \ll 1$, the redshift dependence of the flux can be approximated as

$$\lim_{z\to 0} z^2(1+z)^{1+\alpha} = z^2 \tag{4.33}$$

and thus the approximation for the redshift in this regime is given by

$$z \approx \sqrt{\frac{PH_0^2}{S_\nu}}. \tag{4.34}$$

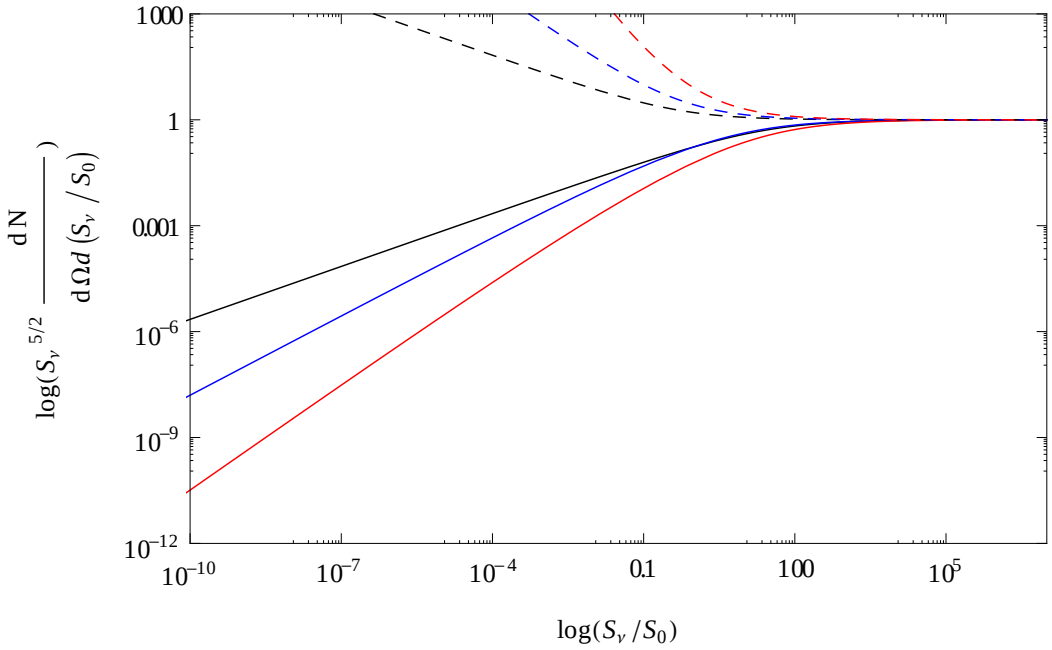

Figure 4.5: Exact solutions and approximations of the specific differential number counts for the de Sitter model for $S_\nu/S_0 \gg 1$. Solid lines are the exact solutions, dashed lines the approximations.
Black: $\alpha = 0$, blue: $\alpha = 1$ (bolometric solution), red: $\alpha = 3$.

Then the flux dependent differential number counts in the limit of low redshifts, i.e. fluxes close to S_0 become

$$\frac{dN}{d\Omega d(S_\nu/S_0)} \approx -\frac{n_0}{H_0^3} \quad \frac{\left(\frac{S_\nu}{S_0}\right)^{-5/2}\left(\left(\frac{S_\nu}{S_0}\right)^{-1/2}+1\right)^{2+\alpha}}{(3+\alpha)\left(\frac{S_\nu}{S_0}\right)^{-1/2}+2}. \tag{4.35}$$

Figure 4.4 shows the approximations for $S_\nu/S_0 \ll 1$ and figure 4.5 for $S_\nu/S_0 \gg 1$ together with the exact solutions from section 4.1.1 corresponding to the same values of the spectral index α for low and high fluxes, respectively. As in the previous plots, the differential number counts are normalised to the Euclidean number counts by multiplication with $S_\nu^{5/2}$. For low fluxes, the approximations for $\alpha = 1$ and $\alpha = 3$ are quite good, only the approximation for $\alpha = 0$ gives a slightly higher value for the differential number counts than the exact solution. If the approximation of the differential number counts for $\alpha = 0$ was normalised such that it yields the right number counts for low fluxes, one would see that the approximations hold up to higher fluxes the smaller the value of the spectral index is. In the range of large S_ν/S_0 the approximations only work for values greater than one. Therefore these approximations only hold for fluxes up to about $S_\nu/S_0 \approx 10^{-5}$ and above one.

4.2.2 Einstein-de Sitter model

As for the de Sitter model before the redshift is approximated for the limits of high and low redshifts seperately. For the limit $z \gg 1$, the redshift dependence of the flux is given by

$$\lim_{z\to\infty}\left(\sqrt{1+z}-1\right)^2(1+z)^\alpha = (1+z)^{1+\alpha}, \tag{4.36}$$

therefore it follows from the equation for the flux, which was given in equation (2.13),

$$\frac{PH_0^2}{4S_\nu} \approx (1+z)^{1+\alpha}, \tag{4.37}$$

and thus

$$1+z \approx \left(\frac{S_0}{4S_\nu}\right)^{\frac{1}{1+\alpha}} \tag{4.38}$$

with $PH_0^2 = S_0$. Then after inserting this result in equation (4.15) and replacing dS_ν by $d(S_\nu/S_0)$ the specific differential number counts yield

$$\frac{dN}{d\Omega d(S_\nu/S_0)} \approx -\frac{16n_0}{H_0^3}\left(\alpha + \frac{1}{1-\left(2\sqrt{\frac{S_\nu}{S_0}}\right)^{-\frac{1}{1+\alpha}}}\right)\left(\frac{1}{2}\sqrt{\frac{S_\nu}{S_0}}\right)^{\frac{7+2\alpha}{1+\alpha}}. \tag{4.39}$$

For small redshifts, the limit for the flux becomes

$$\lim_{z\to 0}\left(\sqrt{1+z}-1\right)^2(1+z)^\alpha = \left(\sqrt{1+z}-1\right)^2, \tag{4.40}$$

i.e. from equation (2.13) it holds

$$\frac{PH_0^2}{4S_\nu} \approx \left(\sqrt{1+z}-1\right)^2, \tag{4.41}$$

and therfore the redshift dependends on the flux as

$$1+z \approx \left(\sqrt{\frac{PH_0^2}{4S_\nu}}+1\right)^2. \tag{4.42}$$

Then for the specific differential number counts in the limit $z \ll 1$ it holds

$$\frac{dN}{d\Omega d(S_\nu/S_0)} \approx -\frac{16n_0}{H_0^3}\frac{\alpha + \frac{1}{1-\left(\frac{1}{2}\sqrt{\frac{S_\nu}{S_0}}+1\right)^{-1}}}{\left(\frac{1}{2}\sqrt{\frac{S_\nu}{S_0}}+1\right)^{7+2\alpha}}. \tag{4.43}$$

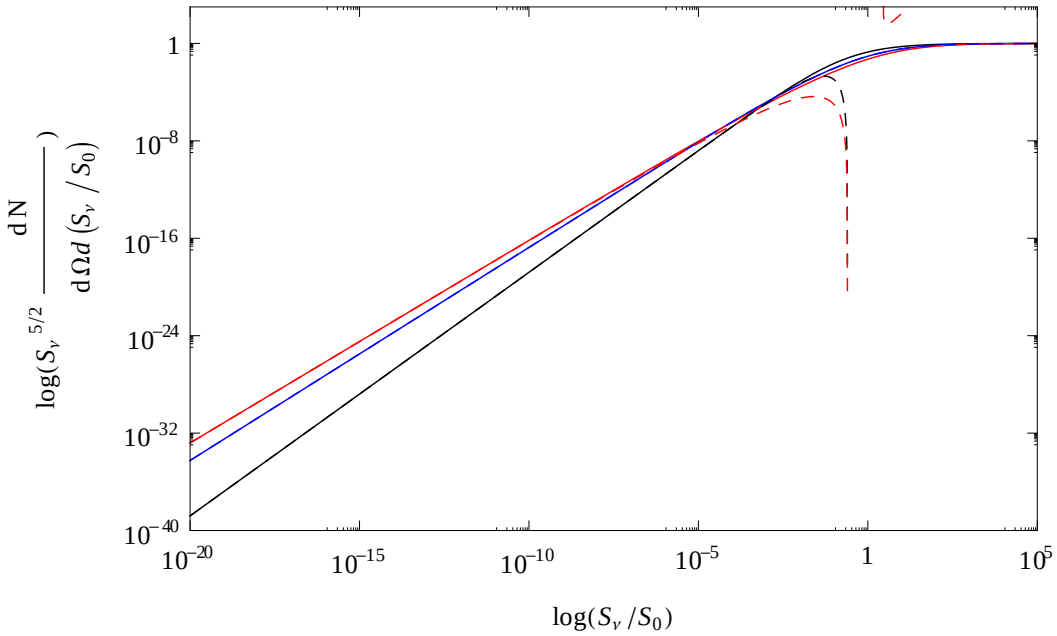

Figure 4.6: Exact solutions and approximations of the specific differential number counts for the Einstein-de Sitter model for $S_\nu/S_0 \ll 1$. Solid lines are the exact solutions, dashed lines the approximations.
Black: $\alpha = 0$, blue: $\alpha = 1$ (bolometric solution), red: $\alpha = 2$.

Figure 4.6 shows the approximations for $S_\nu/S_0 \ll 1$ for the Einstein-de Sitter model together with the exact solutions. As for the de Sitter model before, the number counts are normalised to the Euclidean value. The approximation for the bolometric differential number counts ($\alpha = 1$) is identical with the exact solution because the redshift expressed as a function of the flux is the same. For other values of the spectral index the approximations only work up to a maximal flux and then deviate from the exact differential number counts for the corresponding value of α. It seems that this deviation occurs at lower flux levels the higher the value of the spectral index is. Compared to the approximations for the de Sitter model, the approximations for the Einstein-de Sitter model are even better and work out up to higher fluxes of at least around $S_\nu/S_0 = 10^{-4}$.

In the case of the approximations for $S_\nu/S_0 \gg 1$ shown in figure 4.7, it is that with the spectral index $\alpha = 0$ for which the approximation is identical for all values of the flux. For increasing values of α the slopes of the approximate differential number counts become flatter in the double logarithmic plot and the solution for $\alpha = 2$ evens equals the static Euclidean behaviour. Therefore the approximations for $S_\nu/S_0 \gg 1$ and $\alpha > 0$ coincide with the exact number counts at slightly higher flux levels the greater the spectral index becomes. Contrary to the approximation for high fluxes for the de Sitter model, the approximations for the Einstein-de Sitter model are already close to the exact solutions for $S_\nu/S_0 = 1$.

Approximations for the Einstein-de Sitter model for $S_\nu/S_0 \gg 1$

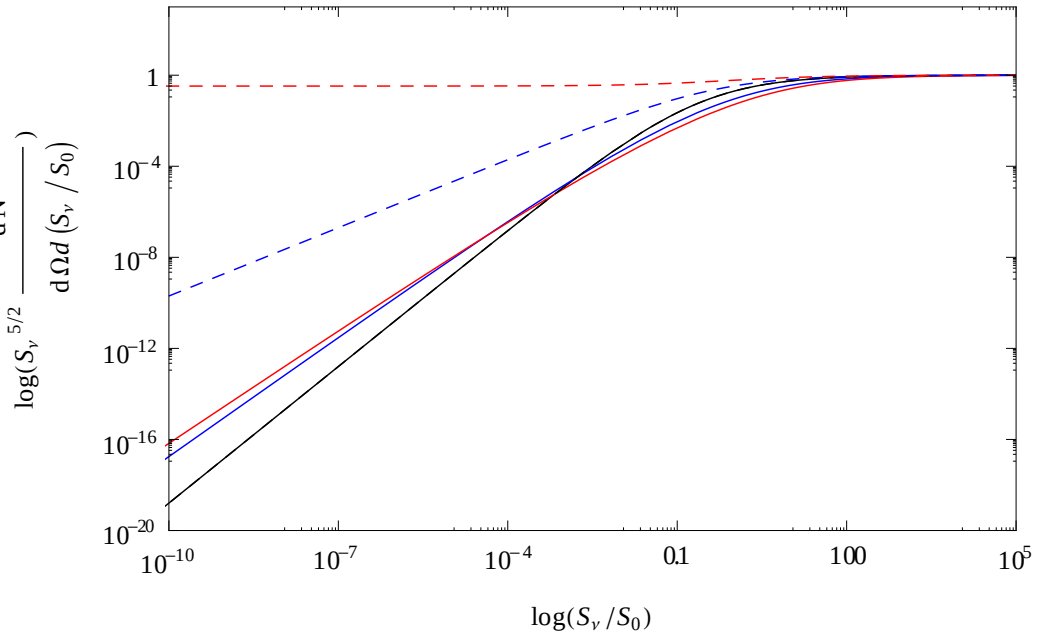

Figure 4.7: Exact solutions and approximations of the specific differential number counts for the Einstein-de Sitter model for $S_\nu/S_0 \gg 1$. Solid lines are the exact solutions, dashed lines the approximations.
Black: $\alpha = 0$, blue: $\alpha = 1$ (bolometric solution), red: $\alpha = 2$.

Thus, the approximations for the Einstein-de Sitter model are better than for the de Sitter model because they are in good agreement to the exact differential number counts for fluxes below $S_\nu/S_0 \approx 10^{-4}$ and above $S_\nu/S_0 \approx 1$.

4.2.3 Milne model

Now the approximated differential number counts will be calculated for the Milne model. Again, the equation for the flux is is approximated for $z \gg 1$ and $z \ll 1$, respectively. In the limit $z \gg 1$ it holds

$$\lim_{z\to\infty} (1+z)^{-1+\alpha} \left((1+z)^2 - 1\right)^2 = (1+z)^{3+\alpha}, \tag{4.44}$$

that is with the equation for the flux eq.(4.21) it follows

$$\frac{4PH_0^2}{S_\nu} \approx (1+z)^{3+\alpha} \tag{4.45}$$

and therefore the redshift is given by

$$1 + z \approx \left(4\frac{PH_0^2}{S_\nu}\right)^{\frac{1}{3+\alpha}}. \tag{4.46}$$

Approximations for the Milne model for $S_\nu/S_0 \ll 1$

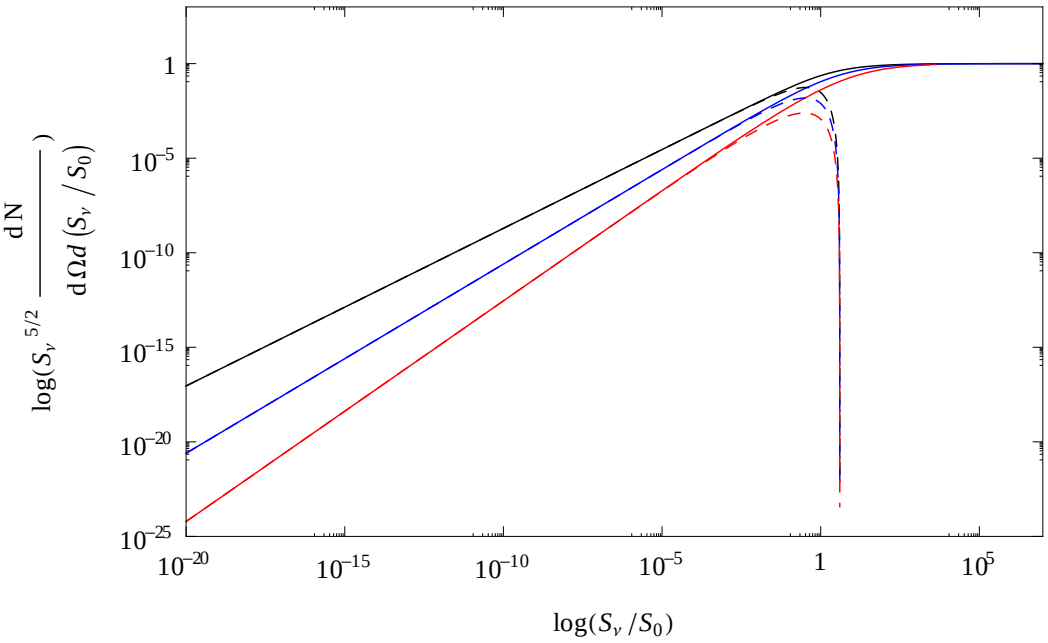

Figure 4.8: Exact solutions and approximations of the frequency dependent differential number counts for the Milne model for $S_\nu/S_0 \ll 1$. Solid lines are the exact solutions, dashed lines the approximations.
Black: $\alpha = 0$, blue: $\alpha = 1$ (bolometric solution), red: $\alpha = 3$.

Regarding these results the flux dependent differential number counts for high redshifts, i.e. low flux become

$$\frac{dN}{d\Omega d(S_\nu/S_0)} \approx \frac{n_0}{16H_0^3} \quad \frac{\left(\left(\frac{S_\nu}{4S_0}\right)^{-\frac{2}{3+\alpha}} - 1\right)^5}{(1-\alpha)\left(\frac{S_\nu}{4S_0}\right)^{-\frac{5-\alpha}{3+\alpha}}\left(1 - \frac{1}{\left(\frac{S_\nu}{4S_0}\right)^{-\frac{2}{3+\alpha}}} - \frac{4}{1-\alpha}\right)}. \tag{4.47}$$

For the limit $z \ll 1$ we have

$$\lim_{z\to 0}(1+z)^{-1+\alpha}\left((1+z)^2 - 1\right)^2 \approx 4z^2 \tag{4.48}$$

which is obtained by a series expansion around zero, thus

$$\frac{PH_0^2}{S_\nu} \approx z^2 \tag{4.49}$$

from eq.(4.21) and then for the redshift it holds

$$z \approx \sqrt{\frac{S_0}{S_\nu}}. \tag{4.50}$$

Figure 4.9: Exact solutions and approximations of the frequency dependent differential number counts for the Milne model for $S_\nu/S_0 \gg 1$. Solid lines are the exact solutions, dashed lines the approximations.
Black: $\alpha = 0$, blue: $\alpha = 1$ (bolometric solution), red: $\alpha = 3$.

Therefore the flux dependent differential number counts in the limit of low redshifts, i.e. high fluxes are given by

$$\frac{dN}{d\Omega d(S_\nu/S_0)} \approx \frac{n_0}{16H_0^3} \frac{\left(\left(1+\frac{1}{\sqrt{\frac{S_\nu}{S_0}}}\right)^2 - 1\right)^5}{(1-\alpha)\left(1+\frac{1}{\sqrt{\frac{S_\nu}{S_0}}}\right)^{5-\alpha}\left(1-\frac{1}{\left(1+\left(\frac{S_\nu}{S_0}\right)^{-1/2}\right)^2}-\frac{4}{1-\alpha}\right)}. \tag{4.51}$$

Figure 4.8 shows the approximations for low fluxes for the Milne model together with the exact solutions calculated in section 4.1. The approximations are in good agreement with the exact differential number counts up to quite high fluxes of about $S_\nu/S_0 \approx 10^{-2}$ or even more. Like for the other models before, the approximations hold up to higher values for the flux for smaller spectral indices.

The approximations for high flux levels are shown in figure 4.9. Here the approximations are also valid for lower fluxes than the approximated differential number counts of the models considered before. Again, the approximations with a small spectral index α fit the number counts best, i.e. work already for lower values of the flux.

Therefore the approximations for the differential number counts for the Milne model are quite good compared to the other two models considered in the previous sections, i.e. they work for a broad flux range.

These results show that the simple approximations are in good agreement with the exact solutions for a broad flux range. Problematic is only the region where S_ν/S_0 lies between about $S_\nu/S_0 \approx 10^{-5}$ and $S_\nu/S_0 \approx 100$ in the case of the de Sitter model. For the Einstein-de Sitter model the approximations are much better and work best for the Milne model except for a flux range of about $10^{-3} < S_\nu/S_0 < 1$. In general, the approximations are better the smaller the spectral index α becomes.

5 Number counts for the Lambda Cold Dark Matter model

One of the most interesting cases for a cosmological model is the Cold Dark Matter model with dark energy (ΛCDM-model) as this corresponds to the current cosmological standard model. The ΛCDM model is a flat model which is dominated by pressureless, non-relativistic matter and a cosmological constant which drives accelerated expansion. Because of its spatial flatness, the following expression for redshift dependent differential number counts can be adapted from equation (2.34) in the third chapter as

$$\frac{dN}{d\Omega dz} = n_0 d_H d_c^2. \tag{5.1}$$

With the Hubble parameter

$$H = H_0\sqrt{\Omega_m(1+z)^3 + \Omega_\Lambda}, \tag{5.2}$$

and $\Omega_\Lambda = 1 - \Omega_m$ for the flat ΛCDM model, the Hubble distance from equation (2.13) and the comoving distance from equation (2.18) this becomes

$$\frac{dN}{d\Omega dz} = \frac{n_0}{H_0^3\sqrt{\Omega_m(1+z)^3 + 1 - \Omega_m}} \left(\int_0^z \frac{dz'}{\sqrt{\Omega_m(1+z')^3 + 1 - \Omega_m}} \right)^2. \tag{5.3}$$

This equation leads to the problem of evaluating the integral which has no analytic solution that can be expressed by elementary functions. Solutions to this integral always contain elliptical or hypergeometric functions and therefore exacerbate further calculations leading to quite complicated formulae. With the substitution $1 + z = x$ and the restrictions that $ztarget = "1" > 0$ and $0 \leq \Omega_m < 1$, the integral has a solution with hypergeometric functions, namely

$$\begin{aligned} &\int_0^z \frac{dz'}{\sqrt{\Omega_m(1+z')^3 + 1 - \Omega_m}} \\ = \; &\frac{2}{\sqrt{\Omega_m}} \left({}_2F_1\left[\frac{1}{6}, \frac{1}{2}, \frac{7}{6}; \frac{\Omega_m - 1}{\Omega_m}\right] - \frac{{}_2F_1\left[\frac{1}{6}, \frac{1}{2}, \frac{7}{6}; \frac{\Omega_m - 1}{\Omega_m(1+z)^3}\right]}{\sqrt{1+z}} \right), \end{aligned} \tag{5.4}$$

where

$${}_2F_1\left[a, b, c; x\right] = \sum_{k=0}^{\infty} \frac{a_k b_k}{c_k} \frac{x^k}{k!}, \tag{5.5}$$

with

$$(q)_n = \begin{cases} 1 & : \quad n = 0 \\ q(q+1)\cdots(q+n-1) & : \quad n > 0 \end{cases} \tag{5.6}$$

Regarding this result, the differential number counts as a function of redshift become

$$\begin{aligned} \frac{dN}{d\Omega dz} &= -\frac{4n_0}{H_0^3 \Omega_m \sqrt{\Omega_m (1+z)^3 + 1 - \Omega_m}} \\ &\quad \cdot \left({}_2F_1\left[\frac{1}{6}, \frac{1}{2}, \frac{7}{6}; \frac{\Omega_m - 1}{\Omega_m}\right] - \frac{{}_2F_1\left[\frac{1}{6}, \frac{1}{2}, \frac{7}{6}; \frac{\Omega_m - 1}{\Omega_m (1+z)^3}\right]}{\sqrt{1+z}} \right)^2 . \end{aligned} \tag{5.7}$$

For obtaining $\frac{dN}{d\Omega dS} = \frac{dN}{d\Omega dz}\frac{dz}{dS}$, the derivative $\frac{dS}{dz}$ must be calculated as for the other models before, where the flux is given by equation (2.22). With the above result for the integral, the changing rate of the flux with redshift is given by

$$\begin{aligned} \frac{dS}{dz} &= -\frac{P H_0^2 \Omega_m}{2} \\ &\quad \frac{{}_2F_1\left[\frac{1}{6}, \frac{1}{2}, \frac{7}{6}; \frac{\Omega_m - 1}{\Omega_m}\right] - \frac{{}_2F_1\left[\frac{1}{6}, \frac{1}{2}, \frac{7}{6}; \frac{\Omega_m - 1}{(1+z)^3 \Omega_m}\right]}{\sqrt{1+z}} + \frac{1}{2(1+z)^{3/2}\sqrt{1 - \frac{\Omega_m - 1}{(1+z)^3 \Omega_m}}}}{(1+z)^3 \left({}_2F_1\left[\frac{1}{6}, \frac{1}{2}, \frac{7}{6}; \frac{\Omega_m - 1}{\Omega_m}\right] - \frac{{}_2F_1\left[\frac{1}{6}, \frac{1}{2}, \frac{7}{6}; \frac{\Omega_m - 1}{(1+z)^3 \Omega_m}\right]}{\sqrt{1+z}} \right)^3} . \end{aligned} \tag{5.8}$$

Inserting the inverse dz/dS in $\frac{dN}{d\Omega dS} = \frac{dN}{d\Omega dz}\frac{dz}{dS}$ yields the differential number counts in the frequency interval dS

$$\begin{aligned} \frac{dN}{d\Omega dS} &= -\frac{8n_0}{P H_0^5 \Omega_m^2 \sqrt{\Omega_m (1+z)^3 + 1 - \Omega_m}} \\ &\quad \frac{(1+z)^3 \left({}_2F_1\left[\frac{1}{6}, \frac{1}{2}, \frac{7}{6}; \frac{\Omega_m - 1}{\Omega_m}\right] - \frac{{}_2F_1\left[\frac{1}{6}, \frac{1}{2}, \frac{7}{6}; \frac{\Omega_m - 1}{\Omega_m (1+z)^3}\right]}{\sqrt{1+z}} \right)^5}{{}_2F_1\left[\frac{1}{6}, \frac{1}{2}, \frac{7}{6}; \frac{\Omega_m - 1}{\Omega_m}\right] - \frac{{}_2F_1\left[\frac{1}{6}, \frac{1}{2}, \frac{7}{6}; \frac{\Omega_m - 1}{\Omega_m (1+z)^3}\right]}{\sqrt{1+z}} + \frac{1}{2(1+z)^{3/2}\sqrt{1 - \frac{\Omega_m - 1}{(1+z)^3 \Omega_m}}}} . \end{aligned} \tag{5.9}$$

Figure 5.1 shows the differential number counts for the ΛCDM-model as a function of flux calculated above (eq. (5.9)) together with the differential number counts for the de Sitter and Einstein-de Sitter model from the third chapter, where n_0, P and H_0 were set one. The graph for $\Omega_m = 1$ correctly reproduces the differential number counts for the Einstein-de Sitter model. Increasing values of Ω_m lead to a further approximation to the de Sitter model up to higher redshifts. Because of the ever increasing effect of the factor $(1+z)^3$ for higher redshifts there is still a strong deviation from the de Sitter model even for small values of Ω_m when z becomes large enough.

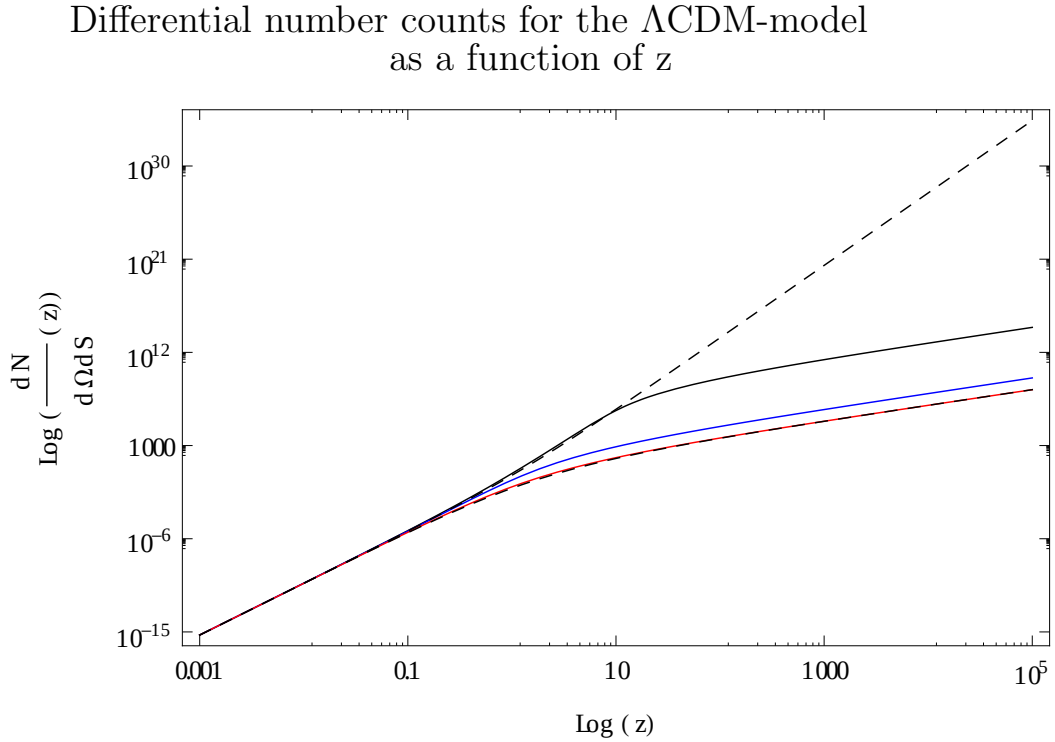

Figure 5.1: Differential number counts for the ΛCDM-model as the function of redshift given in equation (5.9) together with the number counts for the de-Sitter and Einstein-de Sitter model for comparison.
Dashed lines are the differential number counts for the de Sitter model (upper graph) and Einstein-de Sitter model, solid lines are the number counts for the ΛCDM-model.
Black: $\Omega_m = 0.001$, blue: $\Omega_m = 0.3$, red: $\Omega_m = 1$.

The next problem arises when trying to eliminate $1 + z$ from $\frac{dN}{d\Omega dS}$ by solving the formula for the flux for $1+z$ as for the other models before. As this is impossible to solve analytically due to the hypergeometric functions, an approximation becomes necessary. The easiest way to overcome this problem might seem to solve the comoving distance for $z \ll 1$ and $z \gg 1$, which gives the solutions for the de Sitter and Einstein-de Sitter models, respectively. Unfortunately, the value of $\Omega_m = 0$ which corresponds to the de Sitter model whose behaviour is only determined by a cosmological constant, cannot be inserted in the differential number counts as this would give zero for the denominator in the argument of the hypergeometric functions. Nevertheless, the differential number counts from equation (5.9) with the redshift as a function of flux of the Einstein-de Sitter model given in equation (3.20) reproduce the bolometric differential number counts of the Einstein-de Sitter model for $\Omega_m = 1$ which is shown in figure 5.3.

In the double logarithmic plot the Euclidean normalised differential number counts always have the same slope for different values of Ω_m and only tilt to the Euclidean value at different flux levels. Obviously, this approach is not a good approximation to the redshift formula in the ΛCDM model. Nevertheless, approximations for the limit $\Omega_m \to 0$ will always be problematic, for the reason stated above that $\Omega_m = 0$ cannot be inserted in the differential number counts for the ΛCDM model. Even an ever so

small Ω_m will have a large contribution at high redshifts as it is muliplied with $(1+z)^3$ in the Hubble rate.

Other approximations than inserting the $1+z$-dependence of the limiting cases which correspond to the de Sitter and Einstein-de Sitter models, are obtained by expanding the hypergeometric functions in series around zero and infinity for high and low redshifts, respectively.

The series expansion of the solution for the comoving distance around infinity to the first order is given by

$$d_c = \frac{2}{H_0\sqrt{\Omega_m}}\left({}_2F_1\left[\frac{1}{6},\frac{1}{2},\frac{7}{6};\frac{\Omega_m-1}{\Omega_m}\right]-\frac{1}{\sqrt{1+z}}\right)+O\left[\frac{1}{1+z}\right]^{3/2}. \tag{5.10}$$

Therefore it holds

$$\sqrt{\frac{S_0}{S}} \approx \frac{2}{\sqrt{\Omega_m}}\left((1+z)\cdot {}_2F_1\left[\frac{1}{6},\frac{1}{2},\frac{7}{6};\frac{\Omega_m-1}{\Omega_m}\right]-\sqrt{1+z}\right) \tag{5.11}$$

and the redshift as a function of flux is approximately given by

$$\begin{aligned}\sqrt{1+z} &= \frac{1}{2\cdot {}_2F_1\left[\frac{1}{6},\frac{1}{2},\frac{7}{6};\frac{\Omega_m-1}{\Omega_m}\right]} \\ &+ \sqrt{\left(\frac{1}{2\cdot {}_2F_1\left[\frac{1}{6},\frac{1}{2},\frac{7}{6};\frac{\Omega_m-1}{\Omega_m}\right]}\right)^2+\frac{\sqrt{\Omega_m}\sqrt{\frac{S_0}{S}}}{2\cdot {}_2F_1\left[\frac{1}{6},\frac{1}{2},\frac{7}{6};\frac{\Omega_m-1}{\Omega_m}\right]}}.\end{aligned} \tag{5.12}$$

This leads to a general formula for the differential number counts without a specified Ω_m for the ΛCDM model in the limit of high redshifts or low fluxes. This equation is not given here explicitly as it is a very complicated expression which is obtained by just inserting the $1+z$-dependence into equation (5.9). The resulting differential number counts are shown in figure 5.4.

For the case of low redshifts the series expansion to the first order around $z=0$ yields the comoving distance

$$\begin{aligned}d_c &= \frac{z}{H_0\cdot 7\Omega_m^{3/2}} \\ &\cdot\left(3(\Omega_m-1){}_2F_1\left[\frac{7}{6},\frac{3}{2},\frac{13}{6};\frac{\Omega_m-1}{\Omega_m}\right]+7\Omega_m{}_2F_1\left[\frac{1}{6},\frac{1}{2},\frac{7}{6};\frac{\Omega_m-1}{\Omega_m}\right]\right) \\ &+ \quad O[z]^2.\end{aligned} \tag{5.13}$$

The first term simplifies to z/H_0 [15] and thus the comoving distance for $S/S_0 \gg 1$ equals that of the de Sitter model leading to the same redshift as a function of flux which was given in equation (3.20). Thus this approximations corresponds to the differential number counts shown in figure 5.2.

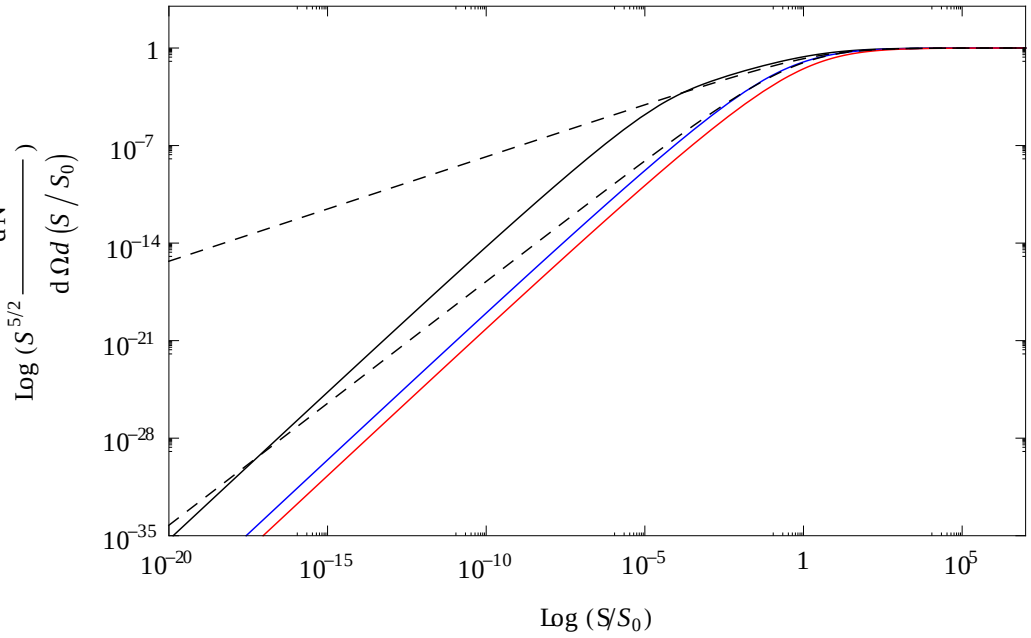

Figure 5.2: Approximations for the differential number counts for the ΛCDM-model for $z = -\frac{1}{2} + \sqrt{\frac{1}{4} + \sqrt{S_0/S}}$ together with the number counts for the de-Sitter and Einstein-de Sitter model for comparison.
Dashed lines are the differential number counts for the de Sitter model (upper graph) and Einstein-de Sitter model, solid lines are the approximations.
Black: $\Omega_m = 0.001$, blue: $\Omega_m = 0.3$, red: $\Omega_m = 1$.

Figure 5.2 shows the differential number counts as a function of flux, i.e. the graphs of equation (5.9) with the redshift obtained for the de Sitter model (equation (3.20)) for the values of the ratio of mass energy to total energy $\Omega_m = 0.001, 0.3$ and 1. Additionally, the bolometric differential number counts of the de Sitter and Einstein-de Sitter models are shown for comparison as these correspond to the limiting cases of $\Omega_m = 0$ and $\Omega_m = 1$, respectively. This approximation leads to graphs which are somewhat steeper than that of the differential number counts for the Einstein-de Sitter model. Higher values of Ω_m yield graphs with the same slope and tilt to the Euclidean slope for S/S_0 close to one. This behaviour is due to the increasing effect of Ω_m for decreasing flux densities as stated above. The approximation of the differential number counts for the ΛCDM model shown in figure 5.3 are obtained by inserting the redshift as a function of flux for the Einstein-de Sitter model into equation (5.7). For $\Omega_m = 1$ this approximation reproduces the differential number counts of the Einstein-de Sitter model as this is identical to a ΛCDM-model with no cosmological constant. It is not surprising that the graphs for $\Omega_m = 0.3$ and $\Omega_m = 0.001$ show the same slope for low flux levels and are shifted to higher numbers as the redshift as a function of flux is simialar to that for the de Sitter model which is shown in figure (5.1). Furthermore, the inserted redshifts leading to figure 5.1 and figure 5.2 do not depend on the value of Ω_m.

ΛCDM-model for the redshift-flux relation of Einstein-de Sitter

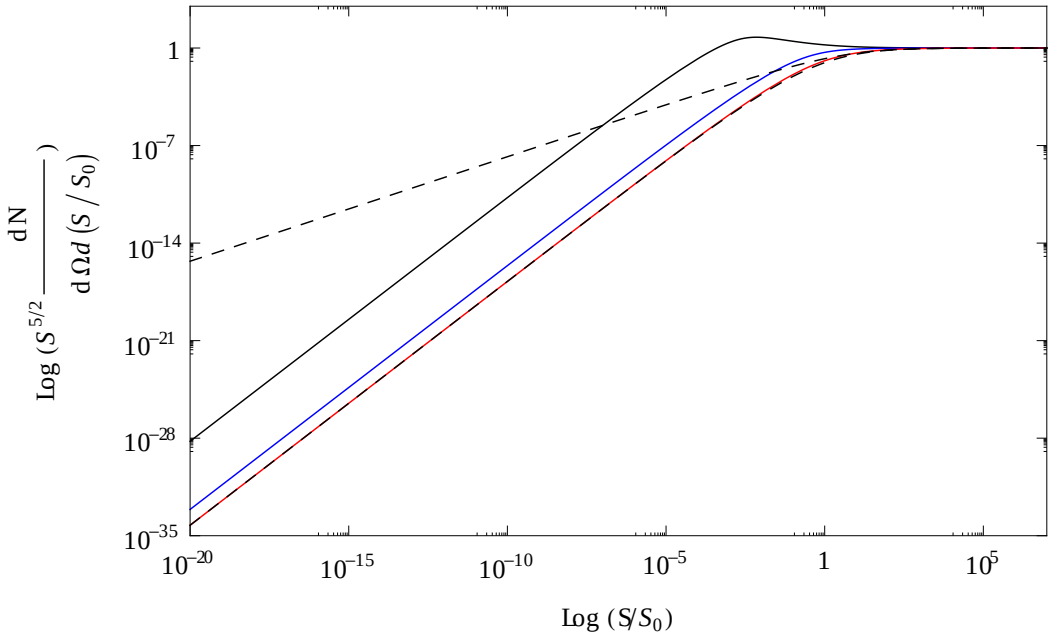

Figure 5.3: Approximations for the differential number counts for the ΛCDM-model for $1+z=\left(\frac{1}{2}+\frac{1}{2}\sqrt{1+2\sqrt{S_0/S}}\right)^2$ together with the number counts for the de-Sitter and Einstein-de Sitter model for comparison.
Dashed lines are the differential number counts for the de Sitter model (upper graph) and Einstein-de Sitter model, solid lines are the approximations.
Black: $\Omega_m = 0.001$, blue: $\Omega_m = 0.3$, red: $\Omega_m = 1$.

Figure 5.4 shows the approximations of the bolometric differential number counts in the ΛCDM-model in the limit $S/S_0 \ll 1$ for values of $\Omega_m = 1, 0.3$ and 0.001. The solutions for $\Omega_m = 1$ and $\Omega_m = 0.3$ are very similar to each other and the approximated differential number counts for $\Omega_m = 1$ coincide with the number counts of the Einstein-de Sitter model. Although the redshift is in this case a function of flux as well as the energy density contributed by matter (or dark energy as $\Omega_m = 1 - \Omega_\Lambda$) the graphs for $\Omega_m = 0.3$ and $\Omega_m = 0.001$ still have the same slope as for the Einstein-de Sitter model. Thus this approximation can only reproduce the differential number counts for the Einstein-de Sitter model and does not approximate the number counts for arbitrary contributions of matter and dark energy. This is again due to the fact that the influence of even a very tiny value of Ω_m has a great contribution to the differential number counts when the flux becomes low enough.

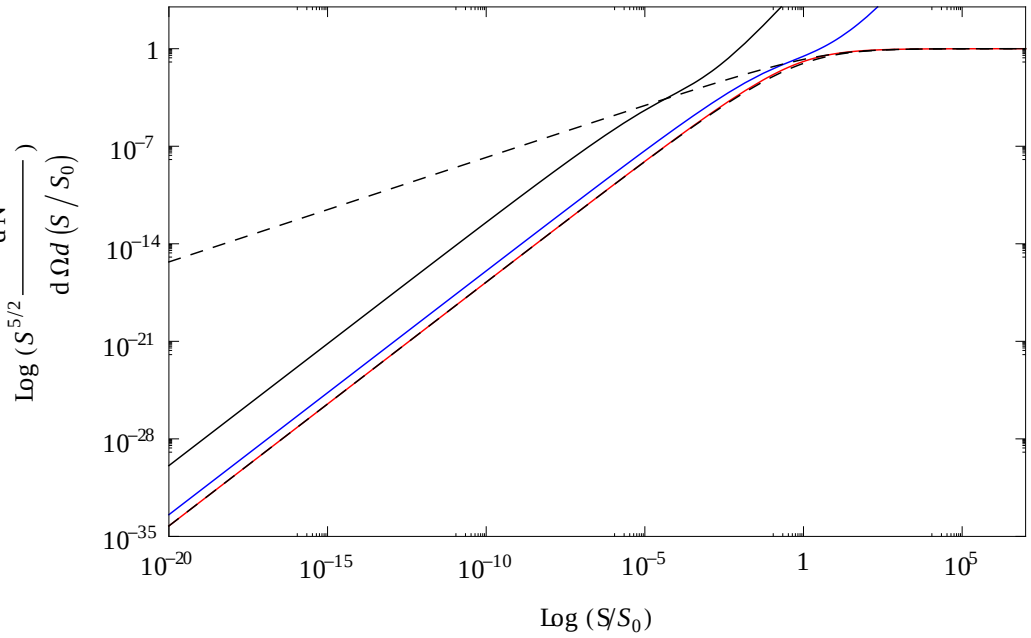

Figure 5.4: Approximations for the differential number counts for the ΛCDM-model for $S/S_0 \ll 1$ together with the number counts for the de-Sitter and Einstein-de Sitter model for comparison.
Dashed lines are the differential number counts for the de Sitter model (upper graph) and Einstein-de Sitter model, solid lines are the approximations.
Black: $\Omega_m = 0.001$, blue: $\Omega_m = 0.3$, red: $\Omega_m = 1$.

These results show that the differential number counts for the ΛCDM-model for non-vanishing values of Ω_m all have the same slope as the Einstein-de Sitter model for low flux densities, i.e. high redshifts. For decreasing contributions of matter to the energy density the differential number counts approach the value for the de Sitter model at higher redshifts or lower flux densities and have the same slope as the number counts for the Einstein-de Sitter model when Ω_m becomes dominant which happens at earlier times the greater the contribution of dark energy becomes. Therefore even very small matter contents lead to the same slope for the differential number counts as in the Einstein-de Sitter model at high redshifts or low flux densities.

6 Conclusion and outlook

The aim of this thesis was to invesigate in how far differential number counts can be calculated analytically for different cosmological models and where approximations become necessary. Furthermore, we wanted to find out which cosmological properties can be actually seen regarding number counts and to which differential number counts are insensitive as a cosmological probe.

All the simple models considered in the third chapter, i.e. the Euclidean and Einstein model as examples for static models, the flat de Sitter model, the Einstein-de Sitter model and the Milne model, can be calculated completely analytical if the differential number counts are not taken to be in a certain frequency band, but bolometric.

Expressing the differential number counts for those models as functions of bolometric flux density could also be done analytical. For the static Einstein model the reference flux density is S_0, corresponding to sources at the "equator" of the 3-sphere. For all other models the reference flux is that of a souce seen at Hubble distance. These calculations can be probably carried out analytical for some other simple models as well, e.g. de Sitter models with $k = \pm 1$. Although these analytic solutions for the differential number counts cannot be applied to surveys as they are bolometric, they are still practical for the investigation of the way in which model properties influence number counts. The main result of this investigation is that number counts model the evolution of the proper volume and hence the Hubble law. Moreover, curvature also leaves an imprint on number counts. At large flux densities, all models agree local Euclidean number counts.

In the fourth chapter the specific differential number counts have been taken into account. The stationary cosmologies have been excluded as flux densities are only redshifted into another frequency band in an expanding (or contracting) universe. Specific number counts in a flux interval dS can be calculated analytically as a function of redshift for the models considered in the third chapter. Expressing the specific differential number counts as a function of flux density is problematic as the flux equation has to be solved for the redshift. This can only be done analytical for specific values of the spectral index α, otherwise approximations become necessary. Simple approximations of the redshift for the limits of $S/S_0 \ll 1$ and $S/S_0 \gg 1$ yield solutions for the specific differential number counts which are in good agreement with the exact solutions that can be obtained for certain values of α for flux densities $S/S_0 \ll 1$ and above one. These approximations improve the smaller the value of the spectral index becomes. It should be possible to find better approximations for the redshift as a function of flux and spectral index that are valid for the range of flux densities between 10^{-5} and one, which could be an issue for further investigation.

Finally, in the fifth chapter the (bolometric) differential number counts have been calculated for the ΛCDM-model, which is spatially flat and its energy density is composed of matter and dark energy (no radiation taken into account). For this model

the differential number counts cannot be expressed in terms of elementary functions. Nevertheless, there is a solution for the flux dependent differential number counts as a function of redshift which contains hypergeometric functions. Approximations similar to those for the specific differential number counts work for low flux densities; the number counts for high flux densities can be approximated best by inserting the redshift as a function of flux for the de Sitter model into the equation for the differential number counts per solid angle $d\Omega$ and flux density interval dS as a function of redshift. These considerations show that even an ever so small amount of energy density contributed by matter results in a slope of the differential number counts equal to that of the Einstein-de Sitter model at early times.

Interesting issues for investigation beyond might be a comparison to numerical calculations. Furthermore, it would be worth to consider the specific differential number counts for the ΛCDM-model. In this work we assumed that all sources have the same isotropic luminosity. An obvious next step would be to include a luminosity distribution and different populations, e.g. two populations with different spectral index. Beyond that, modelling evolution of sources both in density and luminosity and a comparison to data would be worth investigating.

Bibliography

[1] D.L. Jauncey: *Radio surveys and source counts* (Annu. Rev. Astron. Astrophys. 13:23, 1975)

[2] D.F. Crawford, D.L. Jauncey and H.S. Murdoch: *Maximum-Likelihood Estimation of the Slope from Number-Flux Counts of Radio Sources* (Astrophys. J. 162:405, 1970)

[3] S. Chen and D.J. Schwarz: *Fluctuations of differential number counts of radio continuum sources* (February 11, 2015, http://arxiv.org/pdf/1407.4682.pdf)

[4] G. de Zotti, M. Massardi, M. Negrello, and J. Wall: *Radio and Millimeter Continuum Surveys and their Astrophysical Implications* (Astron. Astrophys. Rev. 18, 1, 2010)

[5] M. Massardi, A. Bonaldi, M. Negrello, S. Ricciardi, A. Raccanelli, G. de Zotti: *A model for the cosmological evolution of low frequency radio sources* (Mon. Not. R. Astron. Soc. 404, 532 544, 2010)

[6] V. Mukhanov: *Physical foundations of cosmology* (Cambridge University Press, 2005)

[7] D.S. Gorbunov, V.A. Rubakov: *Introduction to theTheory of the Early Universe: Hot Big Bang Theory.* (World Scientific, 2011)

[8] A. Einstein: *Kosmologische Betrachtungen zur allgemeinen Relativitaetstheorie* (Sitzungsberichte der Kniglich Preuischen Akademie der Wissenschaften (Berlin), pp. 142-152, 1917)

[9] W. de Sitter: *On the relativity of inertia. Remarks concerning Einstein's latest hypothesis* (Koninklijke Nederlandsche Akademie van Wetenschappen Proceedings, vol. 19, iss. 2, 1217-1225, 1916)

[10] H. Bondi, T. Gold: *The Steady-State Theory of the Expanding Universe* (Mon. Not. R. Astron. Soc. vol. 108, 252 270, 1948)

[11] F. Hoyle: *A New Model of the Expanding Universe* (Mon. Not. R. Astron. Soc. vol. 108, 372 382, 1948)

[12] S. Weinberg: *Gravitation and Cosmology: Principals and applications of the General Theory of Relativity* (Wiley, 1972)

[13] A. Einstein, W. de Sitter: *On the Relation between the Expansion and the Mean Density of the Universe* (Proc. Natl. Acad. Sci. USA, vol.18, 1932)

[14] A. Milne: *Relativity, Gravitation and World Structure* (Oxford University Press, 1935)

[15] *Handbook of Mathematical Functions* (pp. 156-158, Dover Publications, New York, 1972)

Statutory Declaration

I declare that I have authored this thesis independently, that I have not used other than the declared sources/resources and that I have explicitly marked all material which has been quoted either literally or by content from the used sources.